Synthesis, in vitro and in vivo biological evaluation of substituted 3-(5-imidazo[2,1-b]thiazolylmethylene)-2-indolinones as new potent anticancer agents

Synthesis, *in vitro* and *in vivo* biological evaluation of substituted 3-(5-imidazo[2,1-*b*]thiazolylmethylene)-2-indolinones as new potent anticancer agents

Rita Morigi,* Alessandra Locatelli, Alberto Leoni, Mirella Rambaldi, Roberta Bortolozzi, Elena Mattiuzzo, Roberto Ronca, Federica Maccarinelli, Ernest Hamel, Ruoli Bai, Andrea Brancale, Giampietro Viola*

European Journal of Medicinal Chemistry, **2019**, 166, 514-530

Synthesis, *in vitro* and *in vivo* biological evaluation of substituted 3-(5-imidazo[2,1-*b*]thiazolylmethylene)-2-indolinones as new potent anticancer agents

Rita Morigi,*[,a] Alessandra Locatelli, [a] Alberto Leoni, [a] Mirella Rambaldi, [a] Roberta Bortolozzi, [b] Elena Mattiuzzo, [b] Roberto Ronca, [c] Federica Maccarinelli, [c] Ernest Hamel, [d] Ruoli Bai, [d] Andrea Brancale, [e] Giampietro Viola*[,b]

[a] *Dipartimento di Farmacia e Biotecnologie Fa.Bi.T, Università di Bologna, 40100 Bologna, Italy*

[b] *Dipartimento di Salute della Donna e del Bambino, Laboratorio di Oncoematologia, Università di Padova, 35131 Padova, Italy*

[c] *Dipartimento di Medicina Molecolare e Traslazionale Unità di Oncologia Sperimentale ed Immunologia, Università di Brescia, 25123 Brescia, Italy;*

[d] *Screening Technologies Branch, Developmental Therapeutics Program, Division of Cancer Treatment and Diagnosis, Frederick National Laboratory for Cancer Research, National Cancer Institute, National Institutes of Health, Frederick, Maryland 21702, USA;*

[e]*The Welsh School of Pharmacy, Cardiff University, Cardiff, CF10 3NB, UK;*

Keywords: Synthesis; 3-(5-imidazo[2,1-*b*]thiazolylmethylene)-2-indolinones; antiproliferative; apoptosis; antitumor.

ABSTRACT

A small library of 3-(5-imidazo[2,1-*b*]thiazolylmethylene)-2-indolinones has been synthesized and screened according to protocols available at the National Cancer Institute (NCI). Some derivatives resulted potent antiproliferative agents, showing GI_{50} values in the nanomolar range. Remarkable, when most active compounds against leukemia cells were tested in human peripheral blood lymphocytes from healthy donors, resulted 100-200 times less cytotoxic. Some compounds, selected by the Biological Evaluation Committee of NCI, were examined to determine tubulin assembly inhibition. Furthermore, flow cytometric studies performed on HeLa, HT-29, and A549 cells, showed that compounds **14** and **25** caused a block in G2/M phase. Interestingly, these derivatives induced apoptosis through the mitochondrial death pathway, causing in parallel significant activation of both caspase-3 and -9, PARP cleavage and down-regulation of the anti-apoptotic proteins Bcl-2 and Mcl-1. Finally, compound **25** was also tested in vivo in the murine BL6-B16 melanoma and E0771 breast cancer cells, causing in both cases a significant reduction of the tumor volume.

Keywords: Synthesis; 3-(5-imidazo[2,1-b]thiazolylmethylene)-2-indolinones; antiproliferative; apoptosis; antitumor.

1. Introduction

Cancer represents a group of diseases which are among the leading causes of morbidity and mortality worldwide, with approximately 14 million new cases and 8.2 million cancer related deaths in 2012 (World Cancer Report 2014). Although considerable progresses in cancer survival has been obtained, particularly for hematopoietic and lymphoid malignancies, these impressive data demonstrate that the development of specific therapies remains an unmet need. Among current anticancer agents, microtubule-targeting molecules have a high therapeutic potential, since they suppress microtubule dynamics, generally causing cell cycle arrest at mitosis in prometaphase, followed by the activation of apoptosis. Anti-microtubule agents interact with tubulin through multiple binding sites. The most extensively studied are the vinca domain, the colchicine site and the α-taxane site [1]. Vinca alkaloids, such as vinblastine, vincristine, and vinorelbine, prevent tubulin polymerization by interacting with a binding site located between two tubulin dimers, interacting almost equally with the α-subunit of one dimer and the β-subunit of the other one. The colchicine site is located at the intradimeric αβ interface of tubulin heterodimers, but the primary interactions of colchicine are with β-tubulin amino acid residues [2]. Some compounds that inhibit colchicine binding to tubulin have more extensive interactions than does colchicine with α-tubulin residues at the dimer interface [3]. The binding site for taxanes and other chemotypes that inhibit [^{3}H]paclitaxel interaction is on the inner surface of polymerized microtubules on the β-subunit. These compounds stabilize microtubule structure and prevents their disassembly.

Despite a variety of antimitotic agents already used in anticancer therapy, drug resistance, toxicity and side effects remain problems to be solved, hence the development of new molecules interacting with microtubules still represents an attractive objective. In this field, our research group published a study concerning new substituted 3-(5-imidazo[2,1-*b*]thiazolylmethylene)-2-indolinones, which were tested for inhibition of tubulin assembly [4]. Considering that the effects on tubulin assembly were modest, compared to their cytotoxic activity, we planned the synthesis of a small library of

new analogs, in order to improve the antiproliferative profile and to further study the mechanism of action.

The new derivatives were obtained by condensing imidazothiazole aldehydes with oxindoles (Scheme 1, Table 1) through the Knoevenagel reaction. This permits the ready synthesis of adducts by reacting an aldehyde with an activated methylene group, thus allowing the generation of a large series of compounds. To create the library, the substituents on the synthons were chosen by taking into consideration the biological results obtained in our previous studies [4,5]. Since derivatives bearing a 2-pyridyl group at the 6 position of the imidazothiazole system showed significant antiproliferative activity, we investigated the effects of shifting the nitrogen in the pyridine system by substituting the 2-pyridyl group with a 3-pyridyl (compounds **3**-**14**) or 4-pyridyl (compounds **15**-**25**) group. Good results were also obtained when the imidazothiazole nucleus was substituted at position 6 with a methoxy group, so a series of derivatives characterized by this feature and bearing the indolinone nucleus with different substituents was prepared (compounds **26**-**37**). Finally, another imidazothiazole nucleus was introduced at the 6 position of the imidazothiazole system (**38**-**52**), in order to study the effects of this bulky heterocycle never used in previously synthesized derivatives.

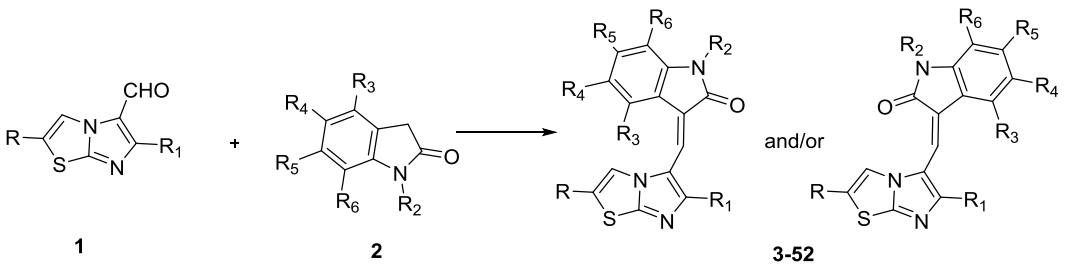

For the substituents see Table 1

Scheme 1. Synthesis of the new 3-(5-imidazo[2,1-*b*]thiazolylmethylene)-2-indolinones.

Table 1. New 3-(5-imidazo[2,1-*b*]thiazolylmethylene)-2-indolinones derivatives and starting compounds

Comp.	Starting compound **1**			Starting compound **2**					
		R	**R_1**		**R_2**	**R_3**	**R_4**	**R_5**	**R_6**
3	**1a**	H		**2a**	H	H	H	H	H
4	**1a**	H		**2b**	CH_3	H	H	H	H
5	**1a**	H		**2c**	H	H	OCH_3	H	H
6	**1a**	H		**2d**	CH_3	H	OCH_3	H	H
7	**1a**	H		**2e**	H	H	OH	H	H
8	**1a**	H		**2f**	CH_3	H	OH	H	H
9	**1a**	H		**2g**	H	H	OCH_3	CH_3	H
10	**1a**	H		**2h**	CH_3	H	OCH_3	CH_3	H
11	**1a**	H		**2i**	H	H	OH	CH_3	H
12	**1a**	H		**2j**	H	H	F	H	H
13	**1a**	H		**2k**	H	H	Cl	H	H
14	**1a**	H		**2l**	H	H	H	CBR	
15	**1b**	H		**2a**	H	H	H	H	H
16	**1b**	H		**2b**	CH_3	H	H	H	H
17	**1b**	H		**2c**	H	H	OCH_3	H	H
18	**1b**	H		**2d**	CH_3	H	OCH_3	H	H
19	**1b**	H		**2e**	H	H	OH	H	H
20	**1b**	H		**2f**	CH_3	H	OH	H	H

21	**1b**	H		**2g**	H	H	OCH_3	CH_3	H
22	**1b**	H		**2h**	CH_3	H	OCH_3	CH_3	H
23	**1b**	H		**2i**	H	H	OH	CH_3	H
24	**1b**	H		**2j**	H	H	F	H	H
25	**1b**	H		**2l**	H	H	H	CBR	
26	**1c**	CH_3	OCH_3	**2a**	H	H	H	H	H
27	**1c**	CH_3	OCH_3	**2b**	CH_3	H	H	H	H
28	**1c**	CH_3	OCH_3	**2n**		H	H	H	H
29	**1c**	CH_3	OCH_3	**2c**	H	H	OCH_3	H	H
30	**1c**	CH_3	OCH_3	**2g**	H	H	OCH_3	CH_3	H
31	**1c**	CH_3	OCH_3	**2e**	H	H	OH	H	H
32	**1c**	CH_3	OCH_3	**2i**	H	H	OH	CH_3	H
33	**1c**	CH_3	OCH_3	**2o**	H	OCH_3	H	H	OCH_3
34	**1c**	CH_3	OCH_3	**2m**	H	OCH_3	OCH_3	OCH_3	H
35	**1c**	CH_3	OCH_3	**2k**	H	H	Cl	H	H
36	**1c**	CH_3	OCH_3	**2p**	H	Cl	H	H	Cl
37	**1c**	CH_3	OCH_3	**2l**	H	H	H	CBR	
38	**1d**	H	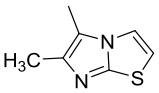	**2a**	H	H	H	H	H
39	**1d**	H	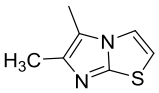	**2c**	H	H	OCH_3	H	H
40	**1d**	H	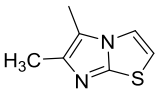	**2k**	H	H	Cl	H	H
41	**1d**	H	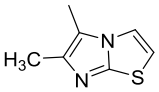	**2q**	H	H	H	Cl	H
42	**1d**	H	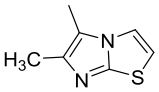	**2l**	H	H	H	CBR	
43	**1e**	CH_3	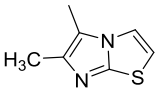	**2b**	CH_3	H	H	H	H

44	**1e**	CH_3	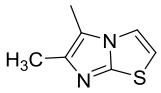	**2n**		H	H	H	H
45	**1e**	CH_3	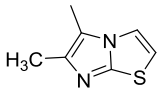	**2c**	H	H	OCH_3	H	H
46	**1e**	CH_3	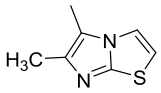	**2g**	H	H	OCH_3	CH_3	H
47	**1e**	CH_3	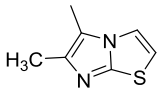	**2e**	H	H	OH	H	H
48	**1e**	CH_3	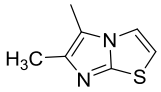	**2j**	H	H	F	H	H
49	**1e**	CH_3	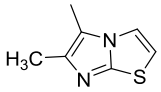	**2k**	H	H	Cl	H	H
50	**1e**	CH_3	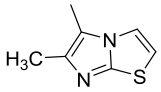	**2r**	H	F	H	H	H
51	**1e**	CH_3	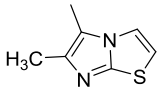	**2s**	H	Cl	H	H	H
52	**1e**	CH_3	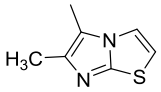	**2q**	H	H	H	Cl	H

CBR = condensed benzene ring

All the new derivatives were evaluated according to protocols available at the National Cancer Institute (NCI, Bethesda, MD). The most active ones were examined to determine the potential inhibition of tubulin assembly and their effects on the binding of [^{3}H]colchicine to tubulin. In addition, the effects of selected compounds on the growth of human peripheral blood lymphocytes derived from healthy donors were assessed. The ability to induce apoptosis in cancer cells was also investigated. Finally, the most active compound was examined for its antitumor activity *in vivo*.

2. Results and discussion

2.1 Chemistry

Compounds **3-52** (Scheme 1 and Table 1) were prepared by means of a single step Knoevenagel reaction between aldehyde **1** and oxindole **2** in methanol/piperidine (33% NH_4OH was

used instead of piperidine for compounds **39**, **41** and **42** to improve the yield). Most derivatives were obtained as pure stereoisomers, but compounds **4**, **12**, **13**, **15**, **16**, **21**, **24**, **25**, **27**, **36**, **39-42**, **44**, **45** and **49** were obtained as *E/Z* mixtures, with the ratio being determined on the basis of the ^{1}H NMR spectra (see Experimental Section). In the case of compound **10**, the two geometrical isomers were obtained and separated by fractional crystallization. In order to determine the geometrical configuration, one isomer was submitted to NOE experiments. The irradiation of the OCH_3 (3.80 ppm) gave NOE at 7.58 ppm, and this singlet was therefore assigned to ind-4. The second experiment enabled the assignment of the geometrical configuration, because irradiation of the singlet at 8.90 ppm (methine bridge) gave NOE at 7.58 ppm (ind-4), which agrees with the *Z* configuration.

By comparing the ^{1}H NMR spectra of the two isomers of compound **10**, it emerged that the ind-4 signal is located in a very different spectral zone. In particular, for the *E* isomer this signal is more shielded (6.04 ppm) than that of the *Z* isomer, which is much more deshielded (7.58 ppm).

We observed that other 3-pyridyl and 4-pyridyl derivatives display this peculiar shift of the ind-4 signal. Therefore, to study the geometrical configuration and this particular behavior, compounds **3**, **5**, **6**, **12**, **14**, **15**, **17**, **19** and **25** were submitted to NOE experiments. Specifically, we investigated the existence of a NOE connection between methine bridge and the ind-4 protons, in fact if a NOE connection is observed, the configuration is *Z*, otherwise it is *E* (Figure 1). Compounds **3**, **5** and **14** gave the results expected of *E* isomers, compounds **6**, **17** and **19** of *Z* isomers, whereas for compounds **12**, **15** and **25**, obtained as mixtures, the most abundant isomer has the *Z* configuration.

The results obtained also confirmed that *E* isomers are characterized by a more shielded ind-4 signal, thus allowing the assignment of the stereochemical configuration of all the other 3-pyridyl and 4-pyridyl derivatives (see Experimental Section). It is interesting to note that the synthesis of the 4-pyridyl derivatives gave pure *Z* isomers or mixtures where the most abundant isomer has the *Z* configuration, whereas most of the 3-pyridyl derivatives has the *E* configuration.

The stereochemical configurations of the derivatives bearing a methoxy group (**26**-**37**) or another imidazothiazole nucleus (**38**-**52**) at the 6 position of the imidazothiazole were also investigated. Compounds **31** and **38** underwent NOE experiments. The results indicated that the configuration is E for both compounds, since no NOE correlation was observed between ind-4 and the methine bridge protons. The configurations of the other analogs were assigned by comparing the ^{1}H NMR spectra. All the derivatives (or the most abundant isomer of the mixture) were *E* isomers (see Experimental Section).

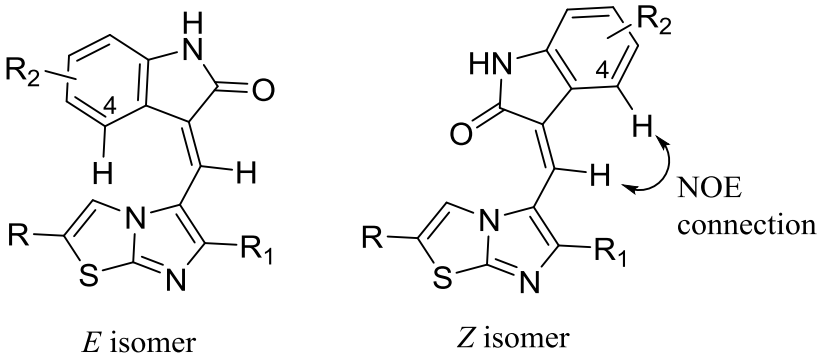

Fig. 1. *E* and *Z* isomers of 3-(5-imidazo[2,1-*b*]thiazolylmethylene)-2-indolinones derivatives.

The two isomers of compound **10** showed very similar antiproliferative profiles, thus confirming that no significant difference is attributable to the stereochemical configuration, as asserted in a previous study [5]. Therefore, compounds obtained as *E*/*Z* mixtures were used without resolving them in the NCI biological assays.

The indolinones **2a**, **2k** and **2q** are commercially available, the other oxindoles and aldehydes were prepared according to the literature [6-21], whereas, the synthesis of new aldehydes **1c**, **1d** and **1e** is reported here. Aldehyde **1c** was obtained from 6-chloro-2-methylimidazo[2,1-*b*]thiazole-5-carbaldehyde (**53**) [22] by treatment with sodium methylate in CH_3OH (Scheme 2). Aldehydes **1d** and **1e** were obtained by means of the Vilsmeier reaction on the corresponding imidazo[2,1-*b*]thiazole (**57d**,**e**), prepared in turn from 2-aminothiazole or 2-amino-5-methylthiazole,

commercially available, and 2-bromo-1-(6-methylimidazo[2,1-*b*]thiazol-5-yl)ethan-1-one (**55**) [23] (Scheme 2).

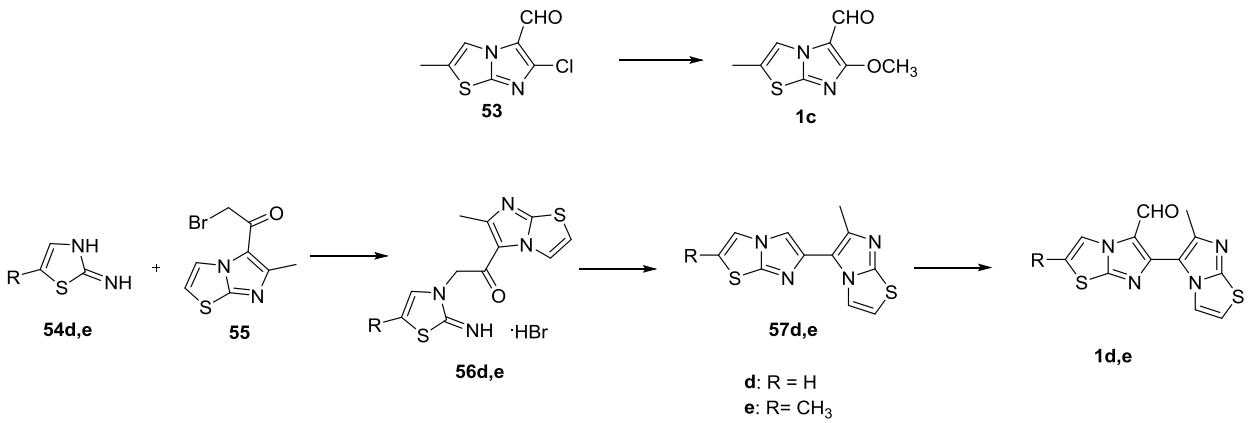

Scheme 2. **Synthesis of the new starting compounds.**

2.2. Biological analysis

2.2.1. In vitro antiproliferative activities

Compounds **3-52** were initially tested at a single high concentration (10^{-5} M) in the full NCI 60 cell panel (NCI 60 Cell One-Dose Screen). This panel is organized into subpanels representing leukemia, melanoma and cancers of the lung, colon, kidney, ovary, breast, prostate and central nervous system. Only compounds that satisfy predetermined threshold inhibition criteria in a minimum number of cell lines progress to the full 5-log concentration assay. The results are expressed as the percentage of growth of treated cells relative to the control following at 48 h incubation. The threshold inhibition criteria for progression were selected to efficiently capture compounds with antiproliferative activity based on analysis of historical Developmental Therapeutics Program (DTP) screening data. Fifteen out of fifty evaluated compounds were active in the preliminary test and progressed to the five-concentration assay, ranging from 10^{-9} to 10^{-4} M.

Table 2 reports the results obtained at three assay endpoints: 50% growth inhibition (GI_{50}), total cytostatic effect (TGI=Total Growth Inhibition) and cytotoxic effect (LC_{50}), determined according to established NCI protocols (http://dtp.nci.nih.gov/branches/btb/ivclsp.html). For some compounds (**15**, **18**, **29** and **37**), the 5-concentration test was repeated, and no significant differences were found between the two assays. For these compounds, the data reported in Table 2 are the mean values of the two experiments.

Table 2. **Nine subpanels at five concentrations: growth inhibition, cytostatic and cytotoxic activity (μM) of selected compounds.**

Comp[a]	Modes	Leu-kemia	NSCLC	Colon	CNS	Mela-noma	Ovarian	Renal	Prostate	Breast	MG-MID[b]
14	GI_{50}	0.11	1.78	0.15	1.16	1.65	1.21	1.24	0.10	0.26	1.02
	TGI	46.42	16.22	9.42	13.90	17.62	12.28	15.88	11.09	20.11	17.81
	LC_{50}	-	61.71	48.99	47.47	66.48	41.22	49.25	33.36	70.82	59.13
15[c]	GI_{50}	2.65	8.97	0.68	1.60	3.27	2.34	14.94	1.10	5.42	5.37
	TGI	91.99	82.42	63.40	49.73	78.34	61.29	73.17	-	67.35	72.47
	LC_{50}	-	-	94.30	94.99	92.25	91.80	92.38	-	-	95.67
18[c]	GI_{50}	0.35	0.55	0.34	0.38	5.97	1.14	0.50	0.39	0.44	1.37
	TGI	81.79	82.43	78.75	63.07	85.27	62.42	65.45	68.75	80.14	74.63
	LC_{50}	96.14	-	92.95	-	-	93.21	-	-	-	97.92
19	GI_{50}	10.08	21.17	7.50	4.46	15.81	33.83	42.97	14.98	4.43	18.64
	TGI	67.60	76.83	93.01	80.43	89.39	86.20	90.10	-	84.17	84.83
	LC_{50}	-	-	-	-	99.11	-	-	-	-	99.86
25	GI_{50}	0.03	11.12	0.03	0.04	7.16	0.05	11.77	0.02	0.04	4.51
	TGI	79.50	79.91	39.94	79.76	72.91	73.84	70.11	55.90	71.26	70.31
	LC_{50}	-	97.87	77.05	94.30	95.26	79.95	-	80.13	99.03	92.50
	GI_{50}	0.50	5.68	0.80	1.97	16.19	6.29	3.53	2.09	2.52	5.17

26	TGI	7.25	65.16	56.75	40.11	74.75	55.65	67.64	45.00	67.30	56.09
	LC_{50}	93.67	99.03	93.26	87.87	94.90	96.31	-	-	-	95.98
27	GI_{50}	4.35	9.50	4.05	9.82	8.08	10.51	13.12	12.60	4.82	8.69
	TGI	74.20	73.21	36.29	42.37	34.21	67.04	70.55	66.65	58.17	56.06
	LC_{50}	-	95.11	91.06	97.32	93.39	92.79	-	-	-	95.84
29[c]	GI_{50}	0.43	1.49	0.32	0.43	3.46	1.32	0.65	0.38	0.87	1.18
	TGI	-	58.65	35.73	33.56	67.65	42.63	61.82	52.78	61.32	57.12
	LC_{50}	-	88.93	79.15	85.44	-	87.59	-	-	-	93.01
30	GI_{50}	-	5.25	42.89	5.70	31.48	7.22	5.81	18.75	4.57	18.34
	TGI	-	74.86	91.70	20.43	91.74	47.10	58.88	-	50.89	67.32
	LC_{50}	-	98.04	-	68.28	-	91.39	90.64	-	91.40	92.95
31	GI_{50}	3.32	7.54	4.79	4.76	4.88	12.85	6.58	7.59	4.57	6.53
	TGI	61.70	71.96	78.20	63.97	38.56	63.45	79.41	96.20	66.17	66.40
	LC_{50}	-	-	98.21	-	94.04	-	-	-	-	98.82
34	GI_{50}	5.73	9.26	6.89	7.79	7.86	13.82	9.36	11.35	5.37	8.70
	TGI	-	58.80	69.89	33.58	65.65	63.24	45.03	-	29.23	56.95
	LC_{50}	-	99.43	97.17	81.40	95.60	92.96	98.25	-	99.32	95.65
37[c]	GI_{50}	0.34	2.82	0.37	0.42	0.52	0.62	1.06	0.30	0.79	0.94
	TGI	84.76	45.34	34.59	38.57	43.31	35.27	38.33	35.25	51.29	43.40
	LC_{50}	-	91.41	71.07	82.92	94.97	91.25	89.60	75.93	-	89.19
38	GI_{50}	35.33	6.72	3.48	3.74	4.81	7.60	7.44	3.48	2.73	6.95
	TGI	-	65.57	17.70	26.91	62.27	61.35	70.29	33.95	22.21	52.43
	LC_{50}	-	97.49	87.44	92.27	84.77	-	94.36	87.65	89.58	92.80
41	GI_{50}	0.77	2.67	1.01	1.94	2.58	3.05	3.06	1.51	1.38	2.11
	TGI	7.28	18.11	12.50	11.69	16.72	21.49	20.30	9.30	13.37	15.37
	LC_{50}	61.91	64.68	54.76	44.50	52.16	75.22	64.68	61.70	72.75	60.42
	GI_{50}	0.15	0.28	0.17	0.21	1.60	0.24	0.26	0.20	0.16	0.43

42	TGI	1.72	8.17	2.82	5.15	7.02	10.16	8.29	4.24	5.88	6.23
	LC_{50}	40.24	39.02	25.95	30.64	26.36	35.17	29.44	15.75	33.16	31.61

[a] Highest conc. = 100 μM, only modes showing a value <100 μM are reported. The compound exposure time was 48 h.

[b] Mean graph midpoint: average value for all cell lines tested; i.e., mean GI_{50}.

[c] Mean of two separate experiments.

The tested compounds showed a mean GI_{50} range between 0.43 and 18.64 μM. Owing to their interesting antiproliferative profiles, compounds **14**, **25**, **26**, **41,** and **42** were submitted to the Biological Evaluation Committee (BEC) of the NCI for possible future development.

Most of the compounds bearing a methyl group at position 2 and a methoxy group at position 6 of the imidazothiazole moiety entered the five-concentration assay. For these derivatives the best results were obtained by introducing a methoxy group at the 5 position of indolinone ring (compound **29**, mean GI_{50} 1.18 μM) and especially if the 6-methoxy-2-methylimidazo[2,1-*b*]thiazole is condensed with the 6,7-benzoindolinone, in fact compound **37** showed in most panels mean GI_{50} values in the submicromolar range. The exploration of indolinone N-methylation led to a reduction of the antiproliferative activity, in fact compound **27** showed a lower cytotoxicity compared to compound **26** (mean GI_{50} 8.69 μM vs. mean GI_{50} 5.17 μM).

The introduction of another imidazothiazole nucleus at the 6 position of the imidazothiazole nucleus did not lead to particular advantages, and resulted detrimental for the activity if the primary imidazothiazole bears also a methyl group at position 2 (compounds **43-52**), in fact none of these derivatives reached the five-concentration assay. Better results were obtained if the biimidazothiazole is condensed with 6-chloro-2-indolinone (compound **41**, mean GI_{50} 2.11 μM) or, even better, with 6,7-benzoindolinone, indeed compound **42** showed good antiproliferative activity, especially against leukemia (mean GI_{50}=0.15 μM), colon (mean GI_{50}=0.17 μM) and breast (mean GI_{50}=0.16 μM) cancer cell lines.

Comparing the series of 3-pyridyl (**3**-**14**) and 4-pyridyl (**15**-**25**) derivatives, better results were obtained with the 4-pyridyl derivatives, in fact a larger number of compounds progressed to the five-concentration assay. Indeed, the only 3-pyridyl derivative active in the NCI 60 cell One-Dose Screen was compound **14** which resulted very active (mean GI_{50}=1.02 μM) and derives from the 6,7-benzoindolinone. Interestingly, compound **25**, obtained by condensing the 6-(pyridin-4-yl)imidazo[2,1-*b*]thiazole-5-carbaldehyde with the 6,7-benzoindolinone showed mean GI_{50} values between 20 and 50 nM for leukemia, colon, CNS, ovarian, prostate and breast panels, thus resulting the most interesting derivative of the series.

Overall these findings appointed the 6,7-benzoindolinone as a useful synthon, which allowed to obtain the most active derivatives either if the 6 position of the imidazothiazole system bears a 3-pyridyl (**14**), a 4-pyridyl (**25**), a methoxy (**37**) group, or another imidazothiazole moiety (**42**).

2.2.2. Effects of test compounds in non-tumor cells

To obtain a preliminary indication of the cytotoxic potential of these derivatives in normal human cells, compounds **14, 25** and **42** were evaluated *in vitro* against peripheral blood lymphocytes (PBL) from healthy donors (Table 3). The three compounds were weakly active in quiescent lymphocytes, having GI_{50} values in the range of 3-33 μM. With the mitogenic stimulus of phytohematoaglutinin (PHA), the GI_{50} values were little changed, except the GI_{50} of compound **42**, which was reduced 2-fold, from 33.2 to 14.9 μM. The GI_{50} values obtained with the lymphocytes were 100-200 times higher than those observed against the leukemia cell lines. These data indicate that the tested derivatives are endowed with a modest effect both in quiescent and in rapidly proliferating normal lymphocytes.

Table 3. Cytotoxicity on human peripheral blood lymphocytes (PBL)

Compound	GI_{50} (μM)[a]	
	$PBL_{resting}$[b]	PBL_{PHA}[c]
14	3.1±0.18	2.5±0.06
25	4.5±0.20	5.5±0.32
42	33.2±3.4	14.9±0.6

[a] Compound concentration required to reduce cell growth inhibition by 50%.

[b] PBL not stimulated with PHA

[c] PBL stimulated with PHA.

Values are the mean ± SEM for three separate experiments.

2.2.3. Inhibition of tubulin polymerization and colchicine binding

On the basis of the NCI 60 Cell Screen data, the BEC proposed some derivatives as possible inhibitors of tubulin polymerization. Therefore, compounds **14**, **25**, **26**, **41** and **42** were tested for potential inhibition of tubulin assembly (Table 4) in comparison with the potent colchicine site agent combretastatin A-4 (CA-4) [24]. Compounds **14**, **26** and **42** inhibited tubulin assembly showing IC_{50} values of 2.2-4.4 μM, with the IC_{50} defined as the concentration of compound that inhibits by 50% the extent of assembly of 10 μM tubulin after a 20 min incubation at 30 °C (the value for CA-4 was 0.64 μM). Compound **25** was moderately active (IC_{50}=14 μM), while compound **41** yielded an IC_{50} > 20 μM, possibly due to poor solubility in the assay solution (0.8 M monosodium glutamate).

Thus, the order of inhibitory effects on tubulin polymerization was **CA-4**>**14**>**26**>**42**>>**25**>>**41**. This order of activity as inhibitors of tubulin assembly does not correlate well with their order of activity as antiproliferative agents.

The compounds were also evaluated for their effects on the binding of [^{3}H]colchicine to tubulin [25] at 5 μM and 50 μM concentrations (Table 4). As in the assembly assay, all the compounds were less potent than CA-4, which in these experiments inhibited colchicine binding by 98%, at the concentration of 5 μM.

Table 4. **Inhibitory effects on tubulin assembly and colchicine binding to tubulin.**

Compound	Tubulin assembly[a]	Colchicine binding[b]	
	IC_{50}±SD (μM)	% inhibition±SD	
		5 μM inhibitor	50 μM inhibitor
14	2.2 ± 0.2	31 ± 5	56 ± 4
25	14 ± 2	25 ± 3	51 ± 2
26	3.4 ± 0.2	39 ± 4	81 ± 0.9
41	> 20	15 ± 9	28 ± 8
42	4.4 ± 0.8	12 ± 3	28 ± 3
CA-4	0.64 ± 0.01	98 ± 1	n.d.

[a] Inhibition of tubulin polymerization. Tubulin was at 10 μM.

[b] Inhibition of [^{3}H]colchicine binding. Tubulin and colchicine were at 1 and 5 μM respectively, whereas the tested compounds were at 5 and 50 μM.

n.d.: not determined

*2.2.4. Compounds **14**, **25**, and **42** induce mitotic arrest of the cell cycle*

The effects of 24 h of treatment with different concentrations of compounds **14, 25** and **42** on cell cycle progression were determined by flow cytometry in HeLa, HT-29, and A549 cells (Figure 2). Compounds **14** and **25** caused a significant G2/M arrest in a concentration-dependent manner, with a rise in G2/M cells occurring at a concentration as low as 50 nM, in particular for

compound **25**, while at higher concentrations more than 80% of the cells were arrested in G2/M for both compounds. The cell cycle arrest in G2/M phase was accompanied by a rapid and significant reduction of the G1 and S phase cells. Compound **42** was less active in inducing G2/M arrest in the three cell lines tested.

14 **25** **42**

HeLa

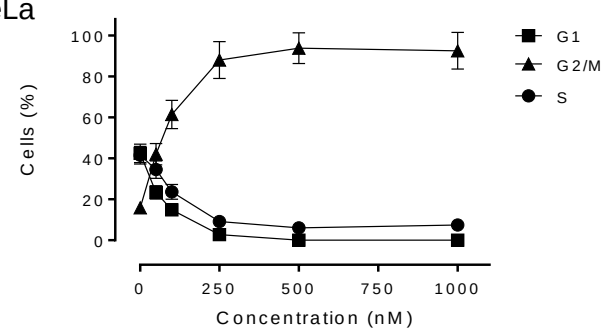

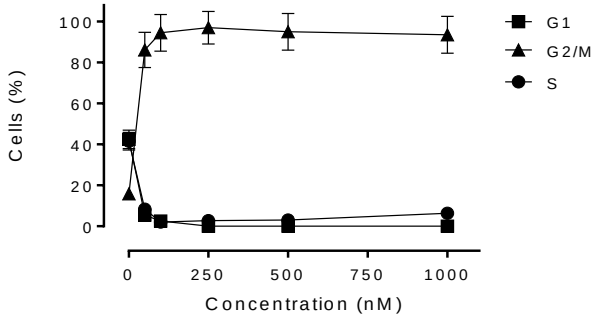

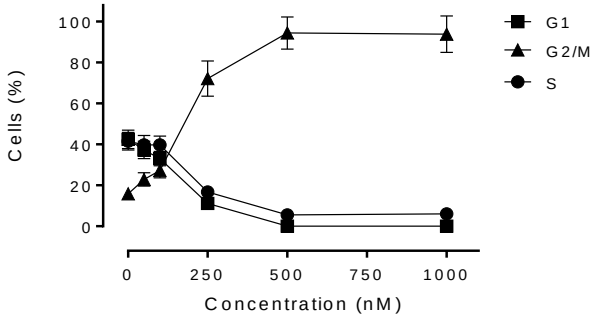

HT-29

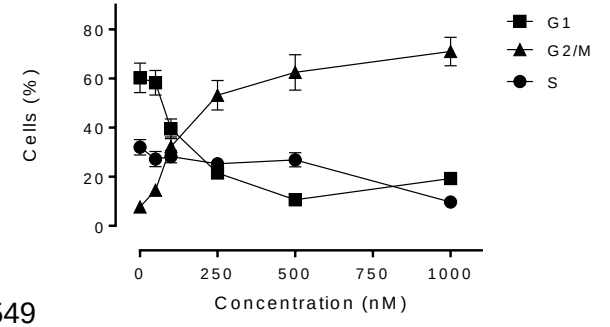

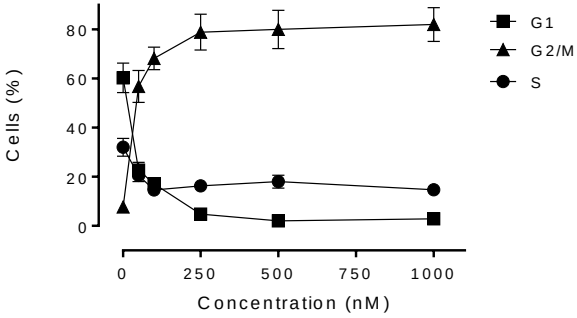

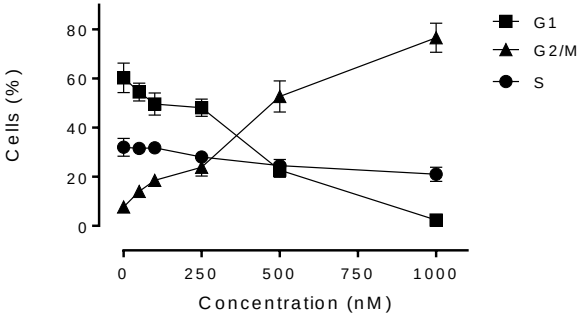

A549

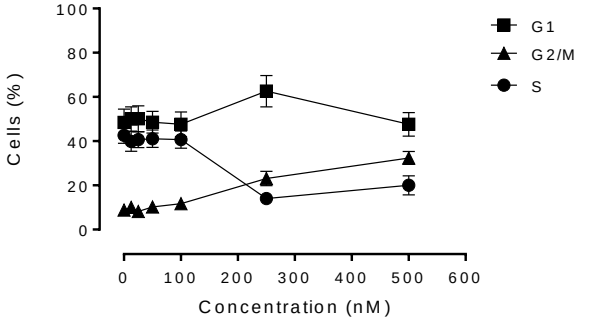

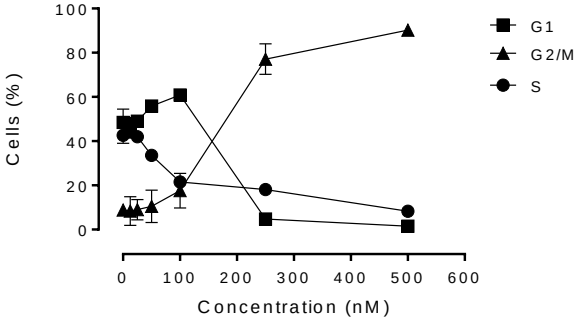

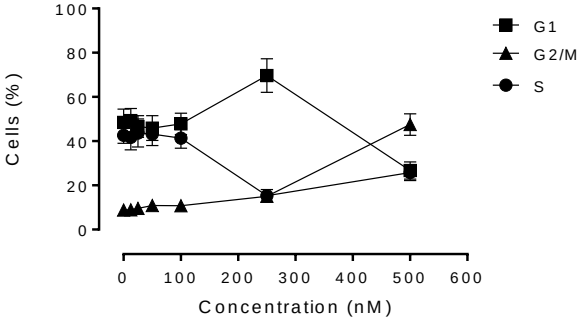

Fig. 2. Percentage of cells in each phase of the cell cycle in HeLa, HT-29 and A549 cells treated with compounds **14**, **25** and **42**, at the indicated concentrations, for 24 h. Cells were fixed and labeled with PI and analyzed by flow cytometry as described in the Experimental Section. Data are shown as mean ± SEM of two independent experiments.

To confirm that the accumulation of G2/M cells was due to mitotic arrest, we evaluated the mitotic index in K562 cells treated at different concentrations with compounds **14**, **25** and **26** and with CA-4 as a positive control. The mitotic index is defined as the number of cells with condensed chromosomes, and indicated as a percentage of the total number of cells. With tubulin-active agents, these are considered cells in prometaphase, as generally there is little or no spindle formation. As shown in Table 5, compounds **14**, **25**, **26** and **CA-4** all caused a marked increase in the mitotic index of K562 cells in comparison to the untreated cells which display a mitotic index of 3%. With all four compounds, this effect increased in a concentration dependent manner.

Table 5. **Mitotic studies with K562 leukemia cells**[a]

Compound	IC_{50} (nM)	Mitotic Index (% of Mitotic cells[b])		
		IC_{50}	5x IC_{50}	10x IC_{50}
14	200	22	64	78
25	30	12	35	58
26	1000	42	61	80
CA-4	4	15	32	61

[a] Cells were grown in RPMI 1640 medium supplemented with 5% fetal bovine serum for 16 h (both for IC_{50} and mitotic index determinations) in a 5% CO_2, humidified atmosphere at 37 °C.

[b] Cells were smeared onto a glass slide, stained with Giemsa, and the proportion of cells with condensed chromosomes was determined. Without compounds the mitotic index was 3%.

We also studied the association between compound-induced G2/M arrest and alterations in G2/M regulatory protein expression in HeLa cells. As shown in Figure 3 (Panels A and B), compounds **14** and **25** caused, in a time- and concentration-dependent manner, an increase in cyclin B1 expression after a 24 h treatment. This was most evident for compound **25**, which caused a significative expression of the protein even at 50 nM, the lowest concentration examined. This effect was confirmed by reduction in the expression of phosphatase cdc25c with both compounds. The phosphorylation of cdc25c directly stimulates its phosphatase activity, and this is necessary to activate cdc2/cyclin B on entry into mitosis [26,27]. In good agreement, we also observed a decrease of the phosphorylated form of cdc2 kinase. Again, compound **25** was the most potent of the two compounds examined. These findings together indicate that the tested compounds cause activation of the mitotic checkpoint following drug exposure.

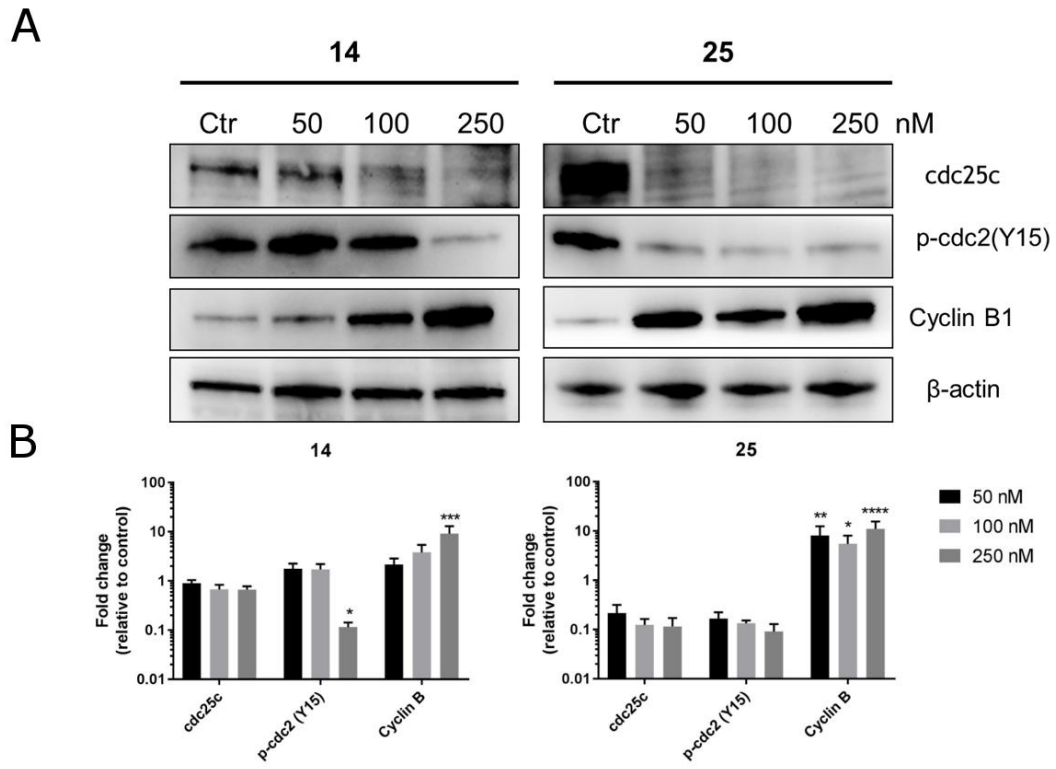

Fig. 3. Effect of compounds **14** and **25** on cell cycle assembly checkpoint proteins. A) Representative immunoblot of HeLa cells treated for 24 h with the indicated concentrations of compounds. The cells were harvested and lysed for detection of the expression of the indicated protein by western blot analysis. To confirm equal protein loading, each membrane was stripped and reprobed with anti-β-actin antibody. B) Densitometric analysis of immunoblots. Each band has been normalized to β-actin and represented as fold change respect to the untreated control. Differences between untreated controls and treated cells were analyzed using one-way ANOVA with Dunnett's multiple comparison test. Data are expressed as mean ± SEM of three independent experiments. *$p<0.05$; **$p<0.01$; ***$p<0.001$

*2.2.5. Compounds **14**, **25** and **42** induced apoptosis through the mitochondrial death pathway*

To evaluate the cell death mode induced by the test compounds, we performed a biparametric cytofluorimetric analysis using propidium iodide (PI) and annexin-V-FITC, which stain DNA and externalized phosphatidylserine (PS) residues, respectively. We examined the ability of the compounds to induce apoptosis at different treatment times and concentrations, using two cell lines, HeLa and A549. In HeLa cells (Figure 4, panels A and B) all three compounds (**14**, **25** and **42)** induced apoptosis in a time- and concentration-dependent manner. In this cell line we used three different concentrations (250, 500 and 1000 nM), and, even at the lowest concentration, it is clear that compound **25** is the most active of the three compounds.

We examined much lower compound concentrations with A549 cells (Figure 5, panels A and B) (12.5-100 nM). At these concentrations, minimal apoptosis occurred with compounds **14** and **42**, even at 100 nM. Compound **25**, however, showed high potency, inducing significant apoptosis even at 25 nM.

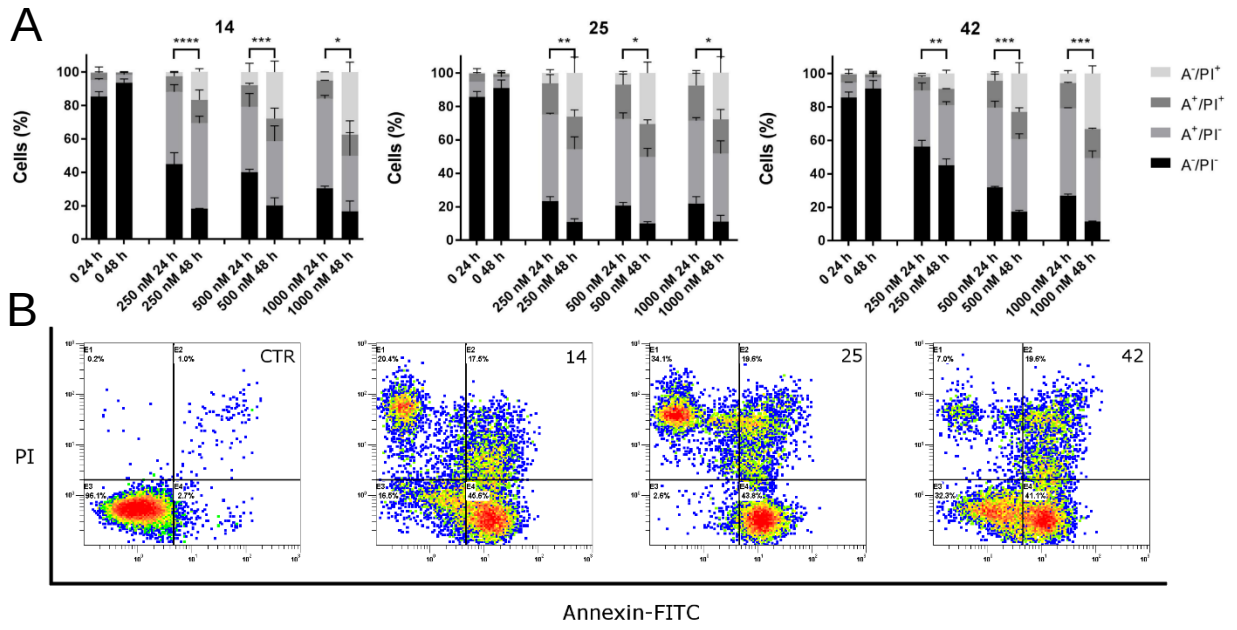

Fig. 4. A) Quantitative analysis of apoptotic cells after treatment of HeLa cells with the test compounds, at the indicated concentrations after incubation for 24 or 48 h. Data are represented as mean ± SEM of three independent experiments. *p<0.05; **p<0.01; ***p<0.001 B) Representative flow cytometric plots of apoptotic cells, after 48 h of treatment with the indicated compounds at the concentration of 250 nM. The cells were harvested and labeled with annexin-V-FITC and PI and analyzed by flow cytometry.

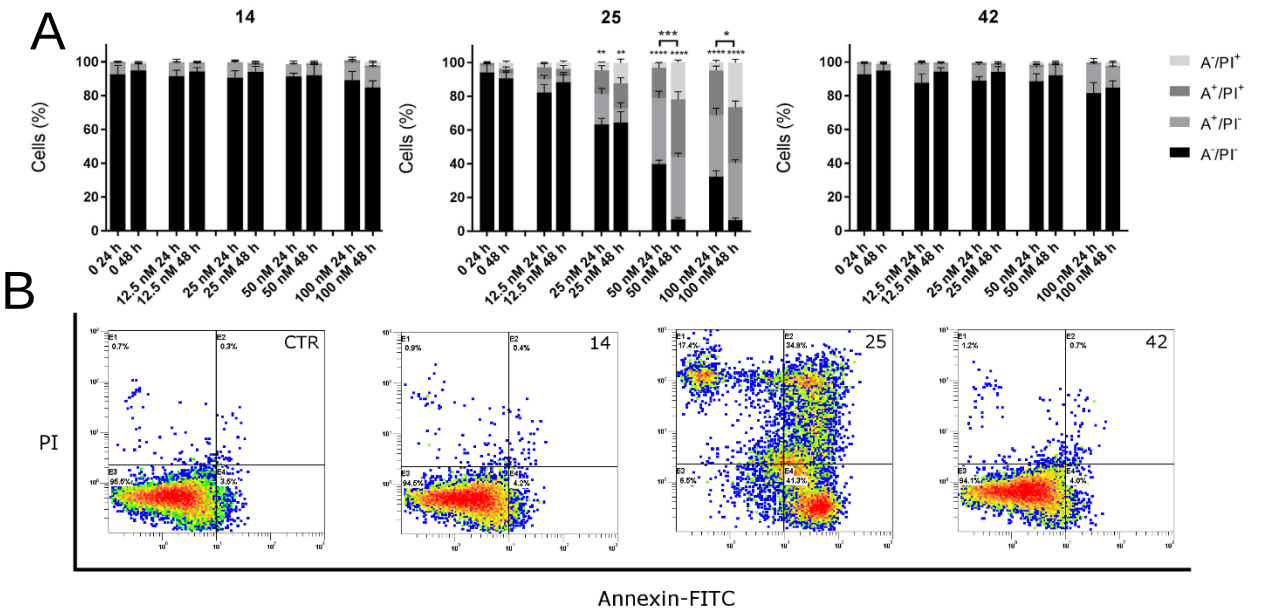

Fig. 5. A) Quantitative analysis of apoptotic cells after treatment of A549 cells with the test compounds, at the indicated concentrations after incubation for 24 or 48 h. Data are represented as mean ± SEM of three independent experiments. *p<0.05; **p<0.01; ***p<0.001 B) Representative flow cytometric plots of apoptotic cells, after 48 h of treatment with the indicated compounds at the concentration of 100 nM. The cells were harvested and labeled with annexin-V-FITC and PI and analyzed by flow cytometry.

Mitochondria play an essential role in the propagation of apoptosis [28,29]. At an early stage, apoptotic stimuli alter the mitochondrial transmembrane potential ($\Delta\psi_{mt}$). We therefore monitored $\Delta\psi_{mt}$ by the fluorescence of the dye JC-1 [30]. HeLa cells treated with compound **14** or **25** (250-500 nM) showed a time-dependent increase in the percentage of cells with low $\Delta\psi_{mt}$ (Figure 6). The depolarization of the mitochondrial membrane is associated with the appearance of annexin-V positivity observed in the experiments described above. In fact, the decrease of $\Delta\psi_{mt}$ is characteristic of apoptosis and has been observed with both microtubule stabilizing and destabilizing agents with a variety of cell types [29,31-33]. Compound **25** resulted the most potent of the two compounds.

Mitochondrial membrane depolarization is associated with mitochondrial production of reactive oxygen species (ROS) [34]. Therefore, we investigated whether ROS production increased after treatment with compounds **14** and **25**. We utilized the fluorescence indicator 2,7-dichlorodihydrofluorescein diacetate (H_2-DCFDA). As shown in Figure 6, both compounds at 250 nM induced significant production of ROS, starting after 12-24 h treatment, in good agreement with the mitochondrial depolarization study described above.

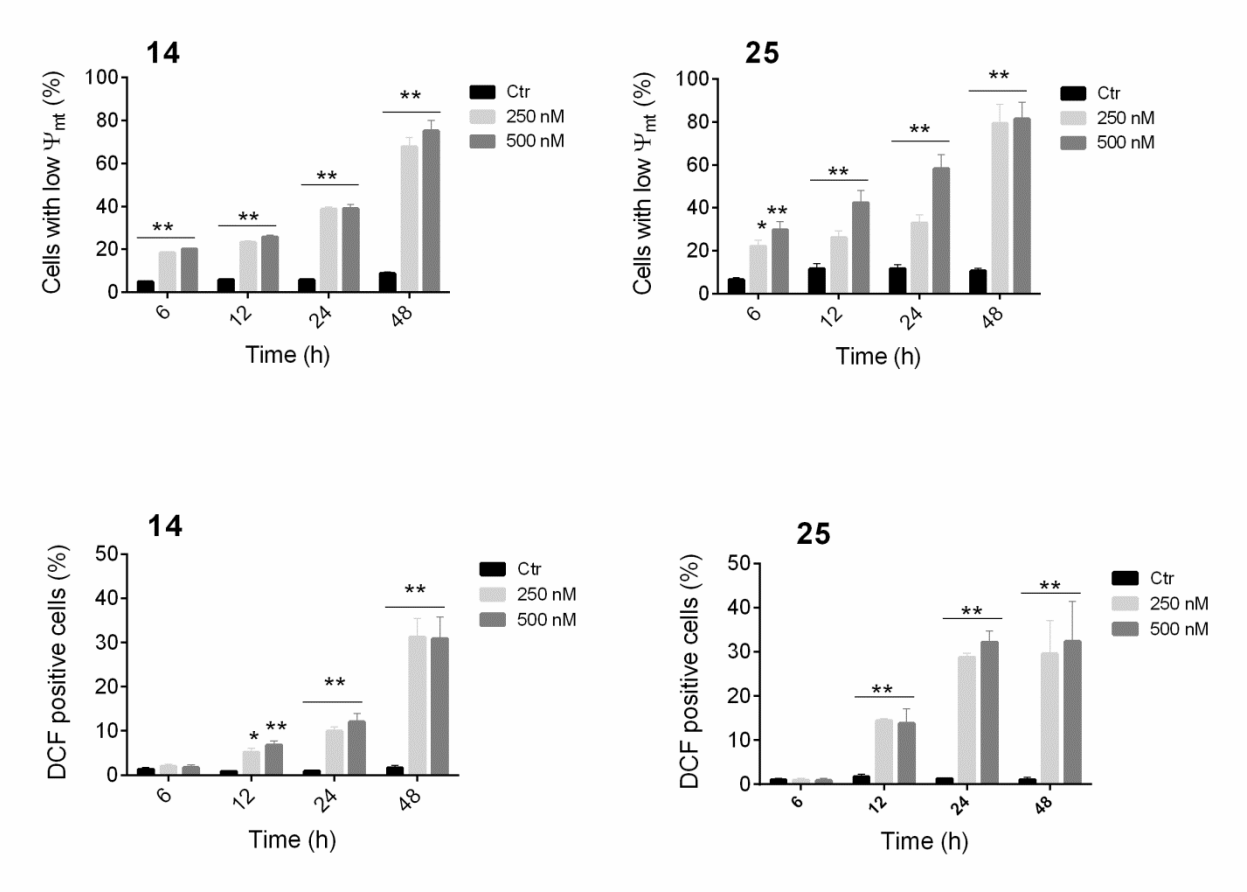

Fig. 6. Assessment of mitochondrial membrane potential ($\Delta\psi_{mt}$) (upper panels) and production of ROS (lower panels) after treatment of HeLa cells with compounds **14** or **25**. Cells were treated with the indicated concentration of compound for 6, 12, 24 or 48 h and then stained with the fluorescent probe JC-1 for analysis of mitochondrial potential or H_2-DCFDA for the evaluation of ROS levels. Cells were then analyzed by flow cytometry as described in the Experimental Section. Data are represented as mean ± SEM of three independent experiments. *p<0.05; **p<0.01 vs control

*2.2.6. Compounds **14** and **25** induce caspase-9, caspase -3, PARP activation and down-regulation of the anti-apoptotic proteins Bcl-2 and Mcl-1.*

To further investigate the apoptotic machinery involved upon treatment of HeLa cells with compounds **14** and **25**, we performed an immunoblot analysis to evaluate the activation of caspase-9 and caspase-3 which are the main caspases involved in mitochondrial apoptosis. As depicted in figure 7 (panels A and B), both caspases are activated after incubation of HeLa cells for 24 h with either compounds. Moreover, the cleavage of poly(ADP-ribose) polymerase (PARP), which is one of the main cleavage targets of caspase-3, occurred with compound **25** even at the lowest concentration used (50 nM), in good agreement with all the other biological assays (Figure 7). We also investigated the expression of two anti-apoptotic proteins, Mcl-1 and Bcl-2 (Figure 7). We and other research groups have shown that sensitivity to antimitotic drugs is regulated by Mcl-1 levels [33,35], a member of the Bcl-2 family of anti-apoptotic proteins. This protein is frequently overexpressed in many cancers and is capable of antagonizing pro-apoptotic proteins and preventing the loss of mitochondrial membrane potential [36]. Bcl-2 is another anti-apoptotic protein that facilitates tumorigenesis and tumor progression [36]. We found that the expression of both Mcl-1 and Bcl-2 was reduced after a 24 h treatment with either compound, while the Mcl-1 was particularly down regulated by treatment with compound **25**.

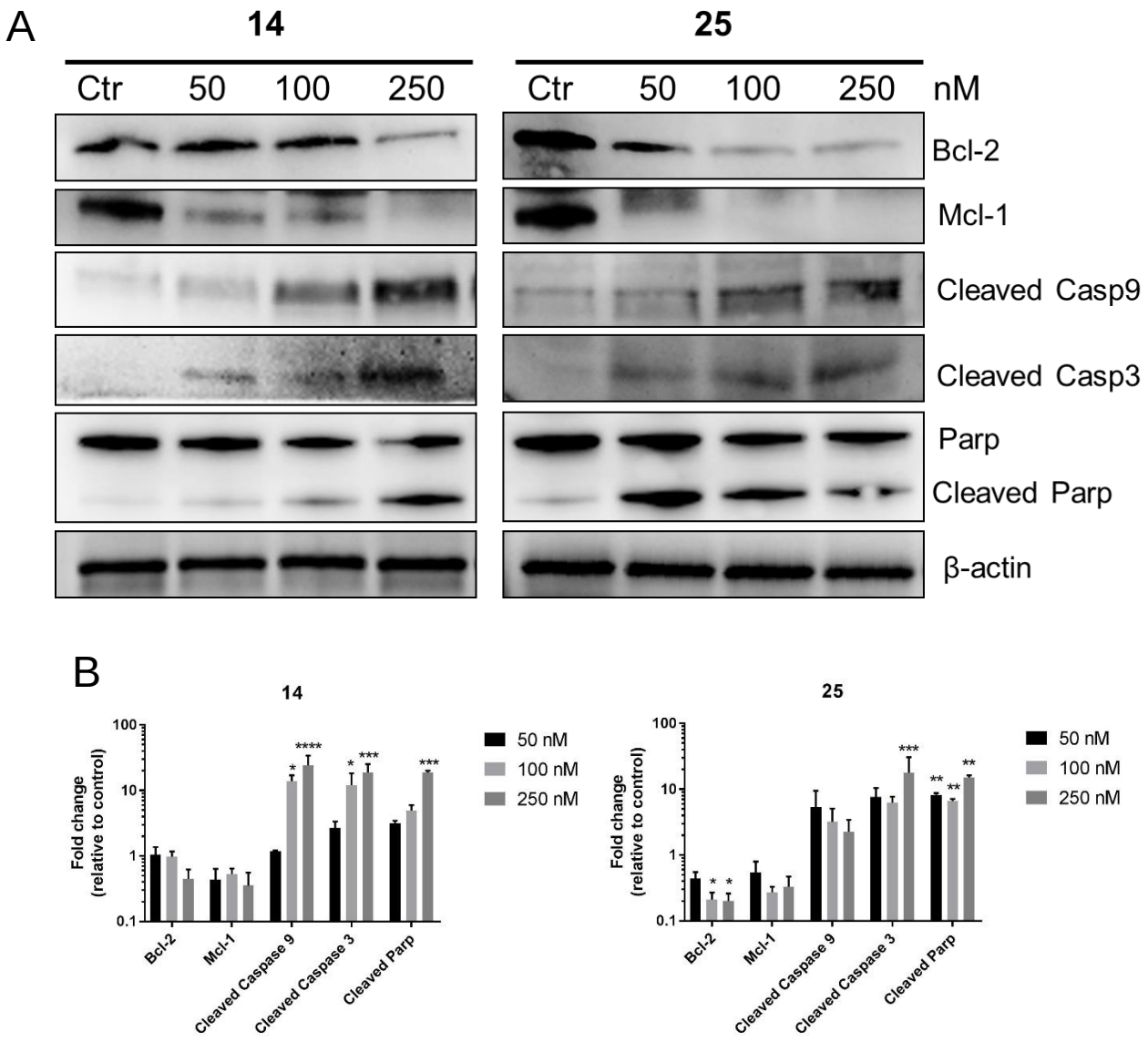

Fig. 7. A) Western blot analysis of Bcl-2, Mcl-1, cleaved Caspase-9, cleaved Caspase-3 and PARP, after treatment of HeLa cells with compounds **14** or **25** at the indicated concentrations for 24 h. To confirm equal protein loading, each membrane was stripped and reprobed with anti-β-actin antibody. B) Densitometric analysis of immunoblots. Each band has been normalized to β-actin and represented as fold change respect to the untreated control. Differences between untreated controls and treated cells were analyzed using one-way ANOVA with Dunnett's multiple comparison test. Data are expressed as mean ± SEM of three independent experiments. *p<0.05; **p<0.01; ***p<0.001

*2.2.7. Evaluation of antitumor activity of compound **25** in vivo.*

To determine the *in vivo* antitumor activity of **25**, two different syngeneic murine models were used [37], represented by the BL6-B16 mouse melanoma cell line and the murine breast cancer cell line EO771. Preliminary *in vitro* experiments were carried out to evaluate the cytotoxicity of compound **25** in both murine tumor cell lines. The GI_{50} obtained after 72 h was 305 ± 45 nM and 15 ± 4.5 nM in BL6-B16 and EO771 cells, respectively.

Both BL6-B16 and E0771 cell lines were injected subcutaneously in syngeneic C57BL/6 mice. Once the tumor reached a measurable size (about 100 mm^3), mice were randomly assigned to different experimental groups and treated intraperitoneally every other day with vehicle (DMSO), compound **25 (**at doses of 7.5 or 15 mg/kg) or with Combretastatin 4-A phosphate (CA-4P) (at 30 mg/kg) as a reference compound.

As shown in Figure 8 (Panel A), compound **25** caused a significant reduction of BL6-B16 melanoma cells growth (29.4%) at the dose of 15 mg/kg, if compared with vehicle-treated group. The reductions observed with 7.5 mg/kg (18%) and CA-4P (16-18%) did not reach statistical significance. Notably, in the E0771 breast cancer model (Figure 8, Panel B), treatment with compound **25** induced a significant reduction of tumor volume at both the doses of 15 mg/kg (56.8% of reduction) and 7.5 mg/kg (51.8% of reduction). Indeed, treatment with the reference compound CA-4P at 30 mg/kg caused only a small reduction in tumor volume (30.9%) if compared with both doses of compound **25**. Under the safety/tolerability point of view, no significant variation in body weight occurred in animals treated with **25** at the higher concentration (data not shown).

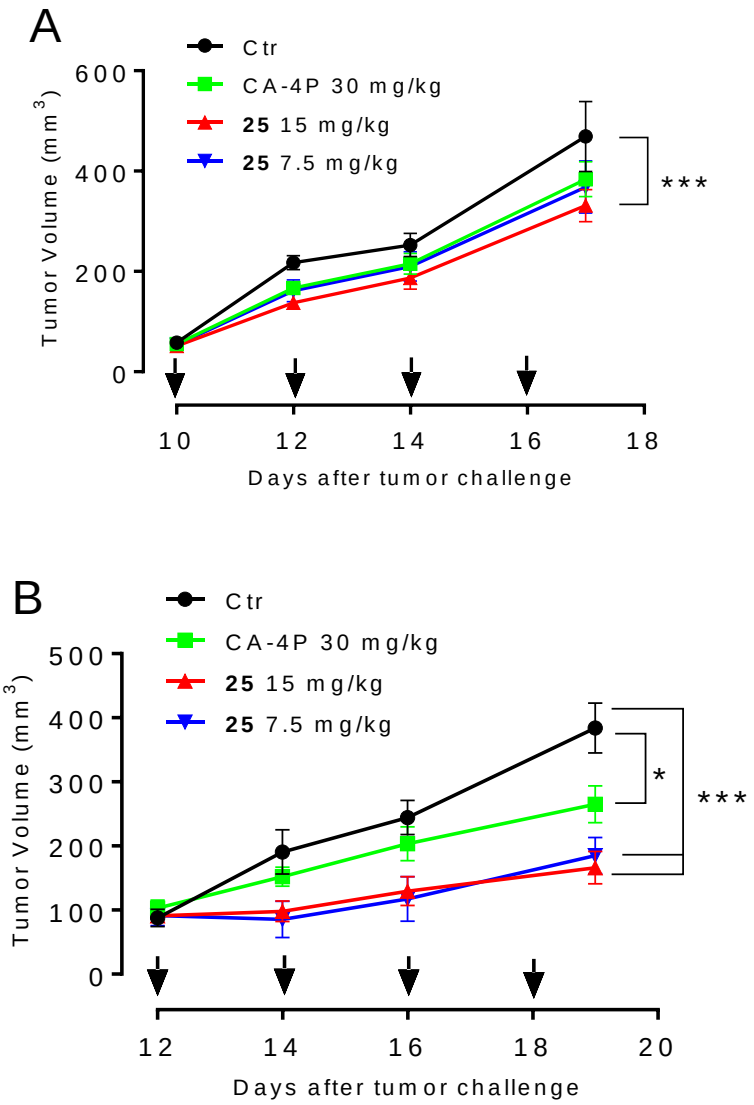

Fig. 8. Inhibition of mouse allograft growth *in vivo* by compound **25**. Male C57BL/6 mice were injected subcutaneously at their dorsal region with 10^7 BL6-B16 murine melanoma cells (Panel A) or EO771 cells (Panel B). Tumor-bearing mice were administered the vehicle, as control, or 15 and 7.5 mg/kg of **25** or CA-4P as reference compound at the dose of 30 mg/kg. Injections were given intraperitoneally at the days indicated by the arrows. Arrows indicate times of administration. Data are presented as mean ± SEM of tumor volume at each time point for 5 animals per group. ***$p<0.01$, *$p<0.05$ *vs*. control.

3. Conclusions

The synthesis of a library composed of fifty new 3-(5-imidazo[2,1-*b*]thiazolylmethylene)-2-indolinones allowed the identification of some derivatives characterized by an interesting antiproliferative profile and GI_{50} values in the nanomolar range. Remarkable, when tested in human peripheral blood lymphocytes from healthy donors, compounds **14**, **25** and **42** resulted 100-200 times less cytotoxic than against leukemia cell lines, showing a modest effect in both quiescent and rapidly proliferating normal lymphocytes. The investigation of the mechanism of action included several studies. First, some derivatives were selected by BEC to determine their effects on tubulin assembly and [^{3}H]colchicine binding, but the inhibition of tubulin polymerization does not correlate perfectly with the antiproliferative activity, and the tested compounds resulted less active than CA-4 in inhibiting colchicine binding. Flow cytometric analysis performed on HeLa, HT-29, and A549 cells, showed that compounds **14** and **25** caused a cell cycle arrest in G2/M phase, attributable to a mitotic arrest, as indicated by the increase of the mitotic index. In addition, compounds **14** and **25** caused in HeLa cells an increase in cyclin B1 expression, more evident for compound **25**. This effect was confirmed by reduction of phosphatase cdc25c expression, and in good agreement, a decrease of the phosphorylated form of cdc2 kinase. These findings are compatible with the activation of the mitotic checkpoint, thus suggesting that these derivatives may interfere with microtubules dynamic. Interestingly, the study of cell death mode proved that compounds **14** and **25** induced apoptosis (**25** even at 25 nM) through the mitochondrial death pathway, causing a strong reduction of the mitochondrial anti-apoptotic proteins Bcl-2 and Mcl-1 expression and in parallel the significant activation of both caspase-9 and -3 and consequent PARP cleavage. Finally, when tested in vivo for its antitumor potential, compound **25** caused a significant reduction of tumor growth on both melanoma (BL6-B16) and breast cancer (E0771) cells, with a therapeutic effect greater than that of CA-4P, the reference compound.

In conclusion, compound **25** emerges as a new effective anticancer drug candidate and as a new lead compound, which may inspire the synthesis of new analogues endowed with even better biological profiles.

4. Experimental section

4.1. Chemical synthesis

The melting points are uncorrected. TLC was performed on Fluka plates (art. 99577) and column chromatography on Silica gel 70-200 μ 60A (Fluorochem): the eluent was a mixture of petroleum ether/acetone in various proportions. Analyses indicated by the symbols of the elements were within ± 0.4% of the theoretical values. The IR spectra were recorded in nujol on a Nicolet Avatar 320 E.S.P.; ν_{max} is expressed in cm^{-1}. The ^{1}H NMR and ^{13}C NMR spectra were recorded on a Varian MR 400 MHz (ATB PFG probe); the chemical shift (referenced to solvent signal) is expressed in δ (ppm) and *J* in Hz (abbreviations: ar=aromatic, ind=indole, py=pyridine, th=thiazole). Compounds **4**, **12**, **13**, **15**, **16**, **21**, **24**, **25**, **27**, **36**, **39-42**, **44**, **45** and **49** were obtained as *E/Z* mixtures, the ratio was determined on the basis of the ^{1}H NMR spectra. The ppm reported in ^{1}H NMR spectra are related to the most prevalent isomer. Only ^{13}C NMR spectra of representative compounds obtained as pure isomers were described.

All solvents and reagents were supplied by Aldrich Chemical Co. Ltd. and were used as supplied. The 2-aminothiazole (**54d**), 2-amino-5-methylthiazole (**54e**), the oxindoles **2a**, **2k** and **2q** are commercially available. The following compounds were prepared according to the literature: **53** [22], **55** [23], **1a-b** [21], **2b** [6], **2c** [7], **2d** [8], **2e** [9], **2f** [8], **2g** [10], **2h** [11], **2i** [12], **2j** [13], **2l** [14], **2m** [15], **2n** [16], **2o** [17], **2p** [18], **2r** [19], and **2s** [20].

*4.1.1. General procedure for the synthesis of compounds **3-52**.*

The appropriate compound **2** (10 mmol) was dissolved in methanol (100 mL) and treated with the equivalent of the appropriate aldehyde **1** and piperidine (1 mL). For compounds **39**, **41** and **42** the yield was much lower (5%), and an improvement (15-20%) was obtained by replacing piperidine with 33% NH_4OH

The reaction mixture was refluxed for 5-10 h, except for compounds **39**-**42** which required a longer reflux time (16-24 h; the progress of the reaction was followed by TLC). The precipitate, formed on cooling, was collected by filtration.

Compounds **39**-**41** were purified by column chromatography with petroleum ether/acetone as the eluent. Most of the crude products were crystallized from methanol, except **27** (acetone/petroleum ether), **34**, **43**-**48**, **50**-**52** (ethanol) and **42**, **49** (toluene). In the case of compound **10**, the two *E*/*Z* isomers were isolated by fractional crystallization from methanol .

*(E)-3-((6-(pyridin-3-yl)imidazo[2,1-b]thiazol-5-yl)methylene)indolin-2-one (**3**).* Yellow solid; 58% yield; mp 298-300 °C. IR cm^{-1} 1700, 1607, 1151, 722. ^{1}H NMR (DMSO-d_6, 400 MHz) δ: 6.43 (1H, d, ind *J*=7.6 Hz), 6.71 (1H, t, ind, *J*=7.6 Hz), 6.87 (1H, d, ind, *J*=7.6 Hz), 7.17 (1H, t, ind, *J*=7.6 Hz), 7.44 (1H, d, th, *J*=4.6 Hz), 7.58 (1H, d, th, *J*=4.6 Hz), 7.66 (1H, s, CH), 8.07 (2H, m, py), 8.48 (1H, m, py), 8.86 (1H, s, py), 10.69 (1H, s, NH). Elemental analysis calcd (%) for $C_{19}H_{12}N_4OS$ (MW 344.39) C 66.26, H 3.51, N 16.27. Found C 66.02, H 3.47, N 16.38.

*1-Methyl-3-((6-(pyridin-3-yl)imidazo[2,1-b]thiazol-5-yl)methylene)indolin-2-one (**4**).* Yellow solid; 47% yield; *E/Z* 19/81; mp 245-247 °C. IR cm^{-1} 1685, 1608, 1258, 743. ^{1}H NMR (DMSO-d_6, 400 MHz) δ: 3.20 (3H, s, N-CH_3), 7.07 (2H, m, ind), 7.35 (2H, m, th+ind), 7.52 (1H, dd, py-5, *J*=8.0, 4.8 Hz), 7.65 (1H, d, th, *J*=4.4 Hz), 7.83 (1H, d, ind, *J*=8.4 Hz), 7.87 (1H, s, CH), 8.09 (1H, d, py-6, *J*=8.0 Hz), 8.58 (1H, s, py-4, *J*=4.8 Hz), 8.89 (1H, d, py-2, *J*=2.0 Hz). Elemental

analysis calcd (%) for $C_{20}H_{14}N_4OS$ (MW 358.42) C 67.02, H 3.94, N 15.63. Found C 67.30, H 4.01, N 15.44.

(E)-5-methoxy-3-((6-(pyridin-3-yl)imidazo[2,1-b]thiazol-5-yl)methylene)indolin-2-one ***(5)****.* Orange solid; 30% yield; mp 305-310 °C. IR cm^{-1} 1711, 1260, 1004, 881. ^1H NMR (DMSO-d_6, 400 MHz) δ: 3.41 (3H, s, O-CH_3), 6.00 (1H, s, ind-4), 6.77 (2H, s, ind), 7.42 (1H, dd, py-5, *J*=7.6, 4.0 Hz), 7.48 (1H, d, th, *J*=4.2 Hz), 7.66 (1H, d, th, *J*=4.2 Hz), 7.69 (1H, s, CH), 8.08 (1H, d, py-6, *J*=7.6 Hz), 8.51 (1H, d, py-4, *J*=4.0 Hz), 8.91 (1H, d, py-2, *J*=2.0 Hz), 10.50 (1H, s, NH). Elemental analysis calcd (%) for $C_{20}H_{14}N_4O2S$ (MW 374.42) C 64.16, H 3.77, N 14.96. Found C 63.98, H 3.88, N 15.01.

(Z)-5-methoxy-1-methyl-3-((6-(pyridin-3-yl)imidazo[2,1-b]thiazol-5-yl)methylene)indolin-2-one ***(6)****.* Red solid; 40% yield; mp 270-280 °C. IR cm^{-1} 1876, 1623, 1125, 820. ^1H NMR (DMSO-d_6, 400 MHz) δ: 3.16 (3H, s, N-CH_3), 3.76 (3H, s, O-CH_3), 6.92 (1H, dd, ind-6, *J*=8.4, 1.8 Hz), 6.96 (1H, d, ind-7, *J*=8.4 Hz), 7.35 (1H, d, th, *J*=4.8 Hz), 7.52 (1H, dd, py-5, *J*=8.0, 4.4 Hz), 7.57 (1H, d, ind-4, *J*=1.8 Hz), 7.62 (1H, d, th, *J*=4.8 Hz), 7.92 (1H, s, CH), 8.09 (1H, d, py-6, *J*=8.0 Hz), 8.58 (1H, d, py-4, *J*=4.8 Hz), 8.89 (1H, d, py-2, *J*=2.4 Hz). Elemental analysis calcd (%) for $C_{21}H_{16}N_4O_2S$ (MW 388.45) C 64.93, H 4.15, N 14.42. Found C 65.00, H 4.28, N 14.22.

(E)-5-hydroxy-3-((6-(pyridin-3-yl)imidazo[2,1-b]thiazol-5-yl)methylene)indolin-2-one ***(7)****.* Red solid; 73% yield; mp >310 °C. IR cm^{-1} 1704, 1263, 1199, 812. ^1H NMR (DMSO-d_6, 400 MHz) δ: 5.96 (1H, d, ind-4, *J*=2.0 Hz), 6.59 (1H, dd, ind-6, *J*=8.0, 2.0 Hz), 6.67 (1H, d, ind-7, *J*=8.0 Hz), 7.46 (2H, m, th+py-5), 7.55 (1H, d, th, *J*=4.4 Hz), 7.59 (1H, s, CH), 8.08 (1H, d, py-6, *J*=8.0 Hz), 8.51 (1H, d, py-4, *J*=4.8 Hz), 8.85 (1H, s, OH), 8.90 (1H, d, py-2, *J*=2.4 Hz), 10.37

(1H, s, NH). Elemental analysis calcd (%) for $C_{19}H_{12}N_4O_2S$ (MW 360.39) C 63.32, H 3.36, N 15.55. Found C 63.54, H 3.47, N 15.25.

(E)-5-hydroxy-1-methyl-3-((6-(pyridin-3-yl)imidazo[2,1-b]thiazol-5-yl)methylene)indolin-2-one ***(8)***. Red solid; 59% yield; mp 296-298 °C. IR cm^{-1} 1690, 1639, 1234, 902. ^1H NMR (DMSO-d_6, 400 MHz) δ: 3.18 (3H, s, N-CH_3), 6.01 (1H, d, ind-4, *J*=2.0 Hz), 6.67 (1H, dd, ind-6, *J*=8.4, 2.0 Hz), 6.84 (1H, d, ind-7, *J*=8.4 Hz), 7.46 (1H, dd, py-5, *J*=8.0, 4.8 Hz), 7.47 (1H, d, th, *J*=4.8 Hz), 7.57 (1H, d, th, *J*=4.8 Hz), 7.68 (1H, s, CH), 8.32 (1H, d, py-6, *J*=8.0 Hz), 8.51 (1H, d, py-4, *J*=4.8 Hz), 8.90 (1H, d, py-2, *J*=2.4 Hz), 8.96 (1H, s, OH). Elemental analysis calcd (%) for $C_{20}H_{14}N_4O_2S$ (MW 374.42) C 64.16, H 3.77, N 14.96. Found C 64.02, H 3.59, N 15.02.

(E)-5-methoxy-6-methyl-3-((6-(pyridin-3-yl)imidazo[2,1-b]thiazol-5-yl)methylene)indolin-2-one ***(9)***. Red solid; 63% yield; mp 249-251 °C. IR cm^{-1} 1704, 1614, 1263, 1193. ^1H NMR (DMSO-d_6, 400 MHz) δ: 2.10 (3H, s, CH_3), 3.30 (3H, s, O-CH_3), 5.99 (1H, s, ind), 6.67 (1H, s, ind), 7.44 (1H, dd, py-5, *J*=8.4, 4.8 Hz), 7.47 (1H, d, th, *J*=4.4 Hz), 7.63 (1H, s, CH), 7.66 (1H, d, th, *J*=4.4 Hz), 8.09 (1H, d, py-6, *J*=8.4 Hz), 8.51 (1H, d, py-4, *J*=4.8 Hz), 8.93 (1H, d, py-2, *J*=2.4 Hz), 10.44 (1H, s, NH). Elemental analysis calcd (%) for $C_{21}H_{16}N_4O_2S$ (MW 388.45) C 64.93, H 4.15, N, 14.42. Found C 65.01, H 4.02, N 14.64.

(Z)-5-methoxy-1,6-dimethyl-3-((6-(pyridin-3-yl)imidazo[2,1-b]thiazol-5-yl)methylene)indolin-2-one ***(10)***. Black solid; 35% yield; mp 264-266 °C. IR cm^{-1} 1690, 1263, 1096, 688. ^1H NMR (DMSO-d_6, 400 MHz) δ: 2.24 (3H, s, CH_3), 3.15 (3H, s, N-CH_3), 3.79 (3H, s, O-CH_3), 6.89 (1H, s, ind), 7.34 (1H, d, th, *J*=4.8 Hz), 7.53 (1H, dd, py-5, *J*=8.0, 4.8 Hz), 7.57 (1H, s, ind), 7.58 (1H, d, th, *J*=4.8 Hz), 7.88 (1H, s, CH), 8.10 (1H, d, py-6, *J*=8.0 Hz), 8.58 (1H, d, py-4, *J*=4.8 Hz),

8.89 (1H, d, py-2, *J*=2.0 Hz). Elemental analysis calcd (%) for $C_{22}H_{18}N_4O_2S$ (MW 402.47) C 65.65, H 4.51, N 13.92. Found C 65.78, H 4.62, 13.99.

(E)-5-methoxy-1,6-dimethyl-3-((6-(pyridin-3-yl)imidazo[2,1-b]thiazol-5-yl)methylene)indolin-2-one ***(10)****.* Dark red solid; 35% yield; mp 244-246 °C. IR cm^{-1} 1702, 1234, 1165, 863. ^1H NMR (DMSO-d_6, 400 MHz) δ: 2.15 (3H, s, CH_3), 3.20 (3H, s, N-CH_3), 3.32 (3H, s, O-CH_3), 6.04 (1H, s, ind), 6.90 (1H, s, ind), 7.45 (1H, dd, py-5, *J*=8.4, 4.8 Hz), 7.48 (1H, d, th, *J*=4.8 Hz), 7.67 (1H, d, th, *J*=4.8 Hz), 7.72 (1H, s, CH), 8.09 (1H, d, py-6, *J*=8.4 Hz), 8.51 (1H, d, py-4, *J*=4.8 Hz), 8.93 (1H, d, py-2, *J*=2.0 Hz). Elemental analysis calcd (%) for $C_{22}H_{18}N_4O_2S$ (MW 402.47) C 65.65, H 4.51, N 13.92. Found C 65.53, H 4.60, N 13.98.

(E)-5-hydroxy-6-methyl-3-((6-(pyridin-3-yl)imidazo[2,1-b]thiazol-5-yl)methylene)indolin-2-one ***(11)****.* Red solid; 68% yield; mp >320 °C. IR cm^{-1} 1710, 1633, 1266, 1186. ^1H NMR (DMSO-d_6, 400 MHz) δ: 2.07 (3H, s, CH_3), 6.03 (1H, s, ind), 6.58 (1H, s, ind), 7.47 (4H, m, 2th+py-5+CH), 8.09 (1H, d, py-6, *J*=8.0 Hz), 8.51 (1H, d, py-4, *J*=4.0 Hz), 8.72 (1H, s, OH), 8.92 (1H, d, py-2, *J*=2.0 Hz), 10.31 (1H, s, NH). Elemental analysis calcd (%) for $C_{20}H_{14}N_4O_2S$ (MW 374.42) C 64.16, H 3.77, N 14.96. Found C 64.56, H 3.84, N 15.01.

5-Fluoro-3-((6-(pyridin-3-yl)imidazo[2,1-b]thiazol-5-yl)methylene)indolin-2-one ***(12)****.* Orange solid; 90% yield; *E/Z* 16/84; mp >310 °C. IR cm^{-1} 1697, 1266, 1156, 803. ^1H NMR (DMSO-d_6, 400 MHz) δ: 6.85 (1H, m, ind), 7.06 (1H, m, ind), 7.37 (1H, d, th, *J*=4.4 Hz), 7.53 (1H, dd, py-5, *J*=7.8, 4.4 Hz), 7.65 (1H, d, th, *J*=4.4 Hz), 7.75 (1H, m, ind), 7.92 (1H, s, CH), 8.10 (1H, d, py-6, *J*=7.8 Hz), 8.60 (1H, d, py-4, *J*=4.4 Hz), 8.90 (1H, d, py-2, *J*=2.4 Hz), 10.59 (1H, s, NH). Elemental analysis calcd (%) for $C_{19}H_{11}FN_4OS$ (MW 362.38) C 62.97, H 3.06, N 15.46. Found C 63.03, H 3.27, N 15.58.

5-Chloro-3-((6-(pyridin-3-yl)imidazo[2,1-b]thiazol-5-yl)methylene)indolin-2-one ***(13)***. Orange solid; 85% yield; *E/Z* 23/77; mp 294-296 °C. IR cm^{-1} 1698, 1264, 1201, 804. ^{1}H NMR (DMSO-d_6, 400 MHz) δ: 6.87 (1H, d, ind-7, *J*=7.8 Hz), 7.27 (1H, dd, ind-6, *J*=7.8, 1.6 Hz), 7.38 (1H, d, th, *J*=4.5 Hz), 7.53 (2H, m, py), 7.66 (1H, d, th, *J*=4.5 Hz), 7.78 (1H, s, py), 7.96 (1H, d, ind-4, *J*=1.6 Hz), 7.98 (1H, s, CH), 8.10 (1H, m, py), 10.70 (1H, s, NH). Elemental analysis calcd (%) for $C_{19}H_{11}ClN_4OS$ (MW 378.83) C 60.24, H 2.93, N 14.79. Found C 60.56, H 2.89, N 14.83.

(E)-3-((6-(pyridin-3-yl)imidazo[2,1-b]thiazol-5-yl)methylene)-1,3-dihydro-2H-benzo[g]indol-2-one ***(14)***. Red solid; 77% yield; mp >310 °C. IR cm^{-1} 1701, 1609, 1254, 1024. ^{1}H NMR (DMSO-d_6, 400 MHz) δ: 6.67 (1H, d, ind, *J*=8.8 Hz), 7.26 (1H, d, ind, *J*=8.8 Hz), 7.42 (1H, dd, py-5, *J*=8.0, 4.8 Hz), 7.44 (1H, d, th, *J*=4.4 Hz), 7.52 (2H, m, ind), 7.69 (1H, d, th, *J*=4.4 Hz), 7.73 (1H, s, CH), 7.81 (1H, m, ind), 8.13 (2H, m, py-6+ind), 8.47 (1H, d, py-4, *J*=4.8 Hz), 8.94 (1H, d, py-2, *J*=2.4 Hz), 11.46 (1H, s, NH). ^{13}C NMR (DMSO-d_6, 100 MHz) δ: 114.9, 115.0, 118.6. 118.8, 119.0, 120.5, 120.6, 120.7, 122.6, 123.8, 126.0, 127.2, 128.3, 128.4, 130.0, 133.7, 134.1, 140.3, 144.6, 147.7, 148.7, 151.9, 169.4. Elemental analysis calcd (%) for $C_{23}H_{14}N_4OS$ (MW 394.45) C 70.03, H 3.58, N 14.20. Found C 70.24, H 3.62, N 14.34.

3-((6-(Pyridin-4-yl)imidazo[2,1-b]thiazol-5-yl)methylene)indolin-2-one ***(15)***. Orange solid; 76% yield; *E/Z* 35/65; mp 310-313 °C. IR cm^{-1} 1707, 1602, 1214, 722. ^{1}H NMR (DMSO-d_6, 400 MHz) δ: 6.88 (1H, d, ind-7, *J*=7.4 Hz), 7.01 (1H, t, ind, *J*=7.4 Hz), 7.27 (1H, t, ind, *J*=7.4 Hz), 7.37 (1H, d, th, *J*=4.5 Hz), 7.65 (1H, d, th, *J*=4.5 Hz), 7.70 (2H, m, py), 7.81 (1H, d, ind-4, *J*=7.4 Hz), 7.88 (1H, s, CH), 8.64 (2H, m, py), 10.61 (1H, s, NH). Elemental analysis calcd (%) for $C_{19}H_{12}N_4OS$ (MW 344.39) C 66.26, H 3.51, N 16.27. Found C 66.15, H 3.59, N 16.38.

1-Methyl-3-((6-(pyridin-4-yl)imidazo[2,1-b]thiazol-5-yl)methylene)indolin-2-one ***(16)***. Orange solid; 70% yield; *E/Z* 31/69; mp 306-307 °C. IR cm^{-1} 1710, 1660, 1598, 722. ^{1}H NMR (DMSO-d_6, 400 MHz) δ: 3.19 (3H, s, N-CH_3), 7.07 (1H, d, ind, *J*=7.6 Hz), 7.09 (1H, t, ind, *J*=7.6 Hz), 7.36 (1H, t, ind, *J*=7.6 Hz), 7.37 (1H, d, th, *J*=4.4 Hz), 7.67 (1H, d, th, *J*=4.4 Hz), 7.68 (1H, d, ind, *J*=7.6 Hz), 7.70 (2H, m, py), 9.94 (1H, s, CH), 8.64 (2H, m, py). Elemental analysis calcd (%) for $C_{20}H_{14}N_4OS$ (MW 358.42) C 67.02, H 3.94, N 15.63. Found C 67.30, H 4.00, N 15.68.

(Z)-5-methoxy-3-((6-(pyridin-4-yl)imidazo[2,1-b]thiazol-5-yl)methylene)indolin-2-one ***(17)***. Dark red solid; 37% yield; mp 290-293 °C. IR cm^{-1} 1701, 1603, 1194, 1025. ^{1}H NMR (DMSO-d_6, 400 MHz) δ: 3.76 (3H, s, O-CH_3), 6.77 (1H, d, ind-7, *J*=8.4 Hz), 6.85 (1H, dd, ind-6, *J*=8.4, 2.0 Hz), 7.36 (1H, d, th, *J*=4.4 Hz), 7.53 (1H, d, ind-4, *J*=2.0 Hz), 7.62 (1H, d, th, *J*=4.4 Hz), 7.70 (2H, d, py, *J*=5.6 Hz), 7.92 (1H, s, CH), 8.65 (2H, d, py, *J*=5.6 Hz), 10.40 (1H, s, NH). Elemental analysis calcd (%) for $C_{20}H_{14}N_4O_2S$ (MW 374.42) C 64.16, H 3.77, N 14.96. Found C 64.34, H 3.81, N 14.86.

(Z)-5-methoxy-1-methyl-3-((6-(pyridin-4-yl)imidazo[2,1-b]thiazol-5-yl)methylene)indolin-2-one ***(18)***. Red orange solid; 70% yield; mp 294-295 °C. IR cm^{-1} 1686, 1600, 1229, 812. ^{1}H NMR (DMSO-d_6, 400 MHz) δ: 3.15 (3H, s, N-CH_3), 3.78 (3H, s, O-CH_3), 6.95 (2H, m, ind), 7.37 (1H, d, th, *J*=4.6 Hz), 7.60 (1H, d, ind-4, *J*=2.0 Hz), 7.64 (1H, d, th, *J*=4.6 Hz), 7.69 (2H, d, py, *J*=5.6 Hz), 7.98 (1H, s, CH), 8.65 (2H, d, py, *J*=5.6 Hz). ^{13}C NMR (DMSO-d_6, 100 MHz) δ: 25.9, 55.7, 107.4, 108.9, 109.5, 112.9, 114.9, 119.4, 120.2, 121.8, 122.7, 123.8, 127.0, 136.7, 140.8, 145.2, 150.0, 155.2, 164.7. Elemental analysis calcd (%) for $C_{21}H_{16}N_4O_2S$ (MW 388.45) C 64.93, H 4.15, N 14.42. Found C 64.88, H 4.09, N 14.55.

*(Z)-5-hydroxy-3-((6-(pyridin-4-yl)imidazo[2,1-b]thiazol-5-yl)methylene)indolin-2-one (**19**).* Dark red solid; 64% yield; mp >320 °C. IR cm^{-1} 1660, 1608, 1194, 763. ^{1}H NMR (DMSO-d_6, 400 MHz) δ: 6.69 (2H, m, ind), 7.19 (1H, d, ind-4, *J*=2.0 Hz), 7.35 (1H, d, th, *J*=4.8 Hz), 7.62 (1H, d, th, *J*=4.8 Hz), 7.69 (2H, dd, py, *J*=5.8, 1.4 Hz), 7.75 (1H, s, CH), 8.64 (2H, dd, py, *J*=5.8, 1.4 Hz), 9.06 (1H, s, OH), 10.30 (1H, s, NH). ^{13}C NMR (DMSO-d_6, 100 MHz) δ: 108.4, 110.0, 112.9, 116.3, 118.4, 120.3, 121.7, 122.5, 124.6, 128.3, 134.2, 141.0, 144.9, 150.0, 151.2, 152.3, 166.5. Elemental analysis calcd (%) for $C_{19}H_{12}N_4O_2S$ (MW 360.39) C 63.32, H 3.36, N 15.55. Found C 63.44, H 3.44, N 15.48.

*(Z)-5-hydroxy-1-methyl-3-((6-(pyridin-4-yl)imidazo[2,1-b]thiazol-5-yl)methylene)indolin-2-one (**20**).* Dark red solid; 67% yield; mp >320 °C. IR cm^{-1} 3389, 1672, 1605, 1003. ^{1}H NMR (DMSO-d_6, 400 MHz) δ: 3.12 (3H, s, N-CH_3), 6.81 (1H, dd, ind-6, *J*=8.4, 2.2 Hz), 6.85 (1H, d, ind-7, *J*=8.4 Hz), 7.27 (1H, d, ind-4, *J*=2.2 Hz), 7.36 (1H, d, th, *J*=4.4 Hz), 7.63 (1H, d, th, *J*=4.4 Hz), 7.69 (2H, dd, py, *J*=6.0, 1.4 Hz), 7.81 (1H, s, CH), 8.64 (2H, dd, py, *J*=6.0, 1.4 Hz), 9.16 (1H, s OH). Elemental analysis calcd (%) for $C_{20}H_{14}N_4O_2S$ (MW 374.42) C 64.16, H 3.77, N 14.96. Found C 64.38, H 3.86, N 14.83.

*5-Methoxy-6-methyl-3-((6-(pyridin-4-yl)imidazo[2,1-b]thiazol-5-yl)methylene)indolin-2-one (**21**).* Brown solid; 50% yield; *E/Z* 15/85; mp 282-284 °C. IR cm^{-1} 1690, 1597, 1122, 722. ^{1}H NMR (DMSO-d_6, 400 MHz) δ: 2.19 (3H, s, CH_3), 3.79 (3H, s, O-CH_3), 6.68 (1H, s, ind), 7.35 (1H, d, th, *J*=4.4 Hz), 7.53 (1H, s, ind), 7.59 (1H, d, th, *J*=4.4 Hz), 7.70 (2H, dd, py, *J*=5.6, 1.6 Hz), 7.87 (1H, s, CH), 8.64 (2H, dd, py, *J*=5.6, 1.6 Hz), 10.35 (1H, s, NH). Elemental analysis calcd (%) for $C_{21}H_{16}N_4O_2S$ (MW 388.45) C 64.93, H 4.15, N 14.42. Found C 64.89, H 4.00, N 14.63.

(Z)-5-methoxy-1,6-dimethyl-3-((6-(pyridin-4-yl)imidazo[2,1-b]thiazol-5-yl)methylene)indolin-2-one ***(22)***. Red orange solid; 39% yield; mp 304-306 °C. IR cm^{-1} 1684, 1599, 1264, 1165. ^1H NMR (DMSO-d_6, 400 MHz) δ: 2.24 (3H, s, CH_3), 3.14 (3H, s, N-CH_3), 3.81 (3H, s, O-CH_3), 6.90 (1H, s, ind), 7.35 (1H, d, th, *J*=4.8 Hz), 7.60 (2H, m, th+ind), 7.70 (2H, dd, py, *J*=6.0, 1.8 Hz), 7.94 (1H, s, CH), 8.64 (2H, dd, py, *J*=6.0, 1.8 Hz). Elemental analysis calcd (%) for $C_{22}H_{18}N_4O_2S$ (MW 402.47) C 65.65, H 4.51, N 13.92. Found C 65.74, H 4.19, N 13.67.

(Z)-5-hydroxy-6-methyl-3-((6-(pyridin-4-yl)imidazo[2,1-b]thiazol-5-yl)methylene)indolin-2-one ***(23)***. Dark red solid; 53% yield; mp >320 °C. IR cm^{-1} 3192, 1690, 1603, 1191. ^1H NMR (DMSO-d_6, 400 MHz) δ: 2.16 (3H, s, CH_3), 6.61 (1H, s, ind), 7.11 (1H, s, ind), 7.34 (1H, d, th, *J*=4.2 Hz), 7.57 (1H, s, CH), 7.59 (1H, d, th, *J*=4.2 Hz), 7.68 (2H, dd, py, *J*=6.0, 1.6 Hz), 8.63 (2H, dd, py, *J*=6.0, 1.6 Hz), 8.93 (1H, s, OH), 10.25 (1H, s, NH). Elemental analysis calcd (%) for $C_{20}H_{14}N_4O_2S$ (MW 374.42) C 64.16, H 3.77, N 14.96. Found C 64.25, H 3.78, N 15.00.

5-Fluoro-3-((6-(pyridin-4-yl)imidazo[2,1-b]thiazol-5-yl)methylene)indolin-2-one ***(24)***. Orange solid; 67% yield; *E/Z* 24/76; mp >320 °C. IR cm^{-1} 1693, 1604, 1193, 778. ^1H NMR (DMSO-d_6, 400 MHz) δ: 6.85 (1H, m, ind), 7.07 (1H, m, ind), 7.38 (1H, d, th, *J*=4.5 Hz), 7.66 (1H, d, th, *J*=4.5 Hz), 7.70 (2H, m, py), 7.78 (1H, m, ind), 7.98 (1H, s, CH), 9.66 (2H, m, py), 10.61 (1H, s, NH). Elemental analysis calcd (%) for $C_{19}H_{11}FN_4OS$ (MW 362.38) C 62.97, H 3.06, N 15.46. Found C 63.02, H 3.45, N 15.55.

3-((6-(Pyridin-4-yl)imidazo[2,1-b]thiazol-5-yl)methylene)-1,3-dihydro-2H-benzo[g]indol-2-one ***(25)***. Red solid; 77% yield; *E/Z* 28/72; mp >320 °C. IR cm^{-1} 1704, 1603, 1182, 1000. ^1H NMR (DMSO-d_6, 400 MHz) δ: 7.40 (1H, d, th, *J*=4.5 Hz), 7.53 (2H, t, ind, *J*=7.2 Hz), 7.58 (1H, d, ind, *J*=8.8 Hz), 7.71 (1H, d, th, *J*=4.5 Hz), 7.74 (2H, dd, py, *J*=7.2, 0.8 Hz), 7.92 (1H, m, ind), 7.97

(1H, d, ind, *J*=8.8 Hz), 7.98 (1H, s, CH), 8.14 (1H, m, ind), 8.65 (2H, dd, py, *J*=7.2, 0.8 Hz), 11.37 (1H, s, NH). Elemental analysis calcd (%) for $C_{23}H_{14}N_4OS$ (MW 394.45) C 70.03, H 3.58, N 14.20. Found C 70.24, H 3.64, N 14.32.

(E)-3-((6-methoxy-2-methylimidazo[2,1-b]thiazol-5-yl)methylene)indolin-2-one ***(26)****.* Yellow orange solid; 64% yield; mp 110-112 °C. IR cm^{-1} 3550-3175, 1690, 1614. ^{1}H NMR (DMSO-d_6, 400 MHz) δ: 2.43 (3H, d, CH_3, *J*=1.3 Hz), 4.01 (3H, s, O-CH_3), 6.84 (1H, d, ind-4/7, *J*=7.6 Hz), 6.97 (2H, m, ind), 7.15 (1H, t, ind-5/6, *J*=7.6 Hz), 7.49 (1H, s, CH), 7.85 (1H, q, th, *J*=1.3 Hz), 10.45 (1H, s, NH). ^{13}C NMR (DMSO-d_6, 100 MHz) δ: 13.3, 56.2, 105.6, 109.0, 117.7, 117.7, 119.4, 120.6, 122.1, 124.6, 125.4, 127.7, 141.7, 147.0, 159.4, 169.2. Elemental analysis calcd (%) for $C_{16}H_{13}N_3O_2S$ (MW 311.36) C 61.72, H 4.21, N 13.50. Found C 61.80, H 4.28, N 13.54.

3-((6-Methoxy-2-methylimidazo[2,1-b]thiazol-5-yl)methylene)-1-methylindolin-2-one ***(27)****.* Yellow solid; 73% yield; *E/Z* 52/48; mp 140-143 °C. IR cm^{-1} 1680, 1603, 1096, 1009. ^{1}H NMR (DMSO-d_6, 400 MHz) δ: 2.43 (3H, s, CH_3), 3.22 (3H, s, N-CH_3), 4.01 (3H, s, O-CH_3), 7.01 (2H, m, ind), 7.23 (1H, m, ind), 7.58 (1H, s, CHO), 7.62 (1H, m, ind), 7.84 (1H, s, th). Elemental analysis calcd (%) for $C_{17}H_{15}N_3O_2S$ (MW 325.39) C 62.75, H 4.65, N 12.91. Found C 62.79, H 4.61, N 11.98

(E)-3-((6-methoxy-2-methylimidazo[2,1-b]thiazol-5-yl)methylene)-1-phenylindolin-2-one ***(28)****.* Orange solid; 60% yield; mp 100-106 °C. IR cm^{-1} 1685, 1603, 1091, 1009. ^{1}H NMR (DMSO-d_6, 400 MHz) δ: 2.44 (3H, s, CH_3), 4.05 (3H, s, O-CH_3), 6.78 (1H, d, ind, *J*=7.4 Hz), 7.13 (3H, m), 7.48 (3H, d, 1Hind *J*=7.4 Hz+2Har), 7.57 (2H, d, ar, *J*=6.6 Hz), 7.70 (1H, s, CH), 7.93 (1H, s, th). Elemental analysis calcd (%) for $C_{22}H_{17}N_3O_2S$ (MW 387.46) C 68.20, H 4.42, N 10.85. Found C 68.34, H 4.52, N 10.91.

(E)-5-methoxy-3-((6-methoxy-2-methylimidazo[2,1-b]thiazol-5-yl)methylene)indolin-2-one ***(29)****.* Red orange solid; 75% yield; mp 128-130 °C. IR cm^{-1} 1698, 1615, 1272, 1213. ^{1}H NMR (DMSO-d_6, 400 MHz) δ: 2.43 (3H, s, CH_3), 3.66 (3H, s, O-CH_3), 4.02 (3H, s, O-CH_3), 6.64 (1H, s, ind), 6.73 (2H, s, ind), 7.49 (1H, s, CH), 7.88 (1H, s, th), 10.26 (1H, s, NH). ^{13}C NMR (DMSO-d_6, 100 MHz) δ: 13.2, 55.4, 56.4, 105.6, 109.2, 110.7, 113.6, 117.6, 117.8, 119.7, 122.9, 125.5, 135.6, 147.1, 154.1, 159.4, 169.3. Elemental analysis calcd (%) for $C_{17}H_{15}N_3O_3S$ (mw 341.39) C 59.81, H 4.43, N 12.31. Found C 59.90, H 4.51, N 12.38.

(E)-5-methoxy-3-((6-methoxy-2-methylimidazo[2,1-b]thiazol-5-yl)methylene)-6-methylindolin-2-one ***(30)****.* Red solid; 56% yield; mp 250-253 °C. IR cm^{-1} 1683, 1603, 1120, 898. ^{1}H NMR (DMSO-d_6, 400 MHz) δ: 2.16 (3H, s, CH_3), 2.43 (3H, s, CH_3), 3.67 (3H, s, O-CH_3), 4.03 (3H, s, O-CH_3), 6.65 (2H, s, ind), 7.41 (1H, s, CH), 7.82 (1H, s, th), 10.20 (1H, s, NH). ^{13}C NMR (DMSO-d_6, 100 MHz) δ: 13.2, 16.5, 55.4, 56.4, 105.5, 108.1, 111.1, 116.5, 117.6, 120.1, 120.3, 125.4, 125.7, 135.5, 146.7, 151.9, 159.2, 169.5. Elemental analysis calcd (%) for $C_{18}H_{17}N_3O_3S$ (MW 355.41) C 60.83, H 4.82, N 11.82. Found C 6091, H 4.92, N 11.89.

(E)-5-hydroxy-3-((6-methoxy-2-methylimidazo[2,1-b]thiazol-5-yl)methylene)indolin-2-one ***(31)****.* Red orange solid; 63% yield; mp 277-278 °C. IR cm^{-1} 3346, 1663, 1583, 1521. ^{1}H NMR (DMSO-d_6, 400 MHz) δ: 3.41 (3H, s, CH_3), 4.01 (3H, s, O-CH_3), 6.55 (2H, m, ind), 6.65 (1H, m, ind), 7.43 (1H, s, CH), 7.81 (1H, s, th), 8.80 (1H, s, OH), 10.10 (1H, s, NH). ^{13}C NMR (DMSO-d_6, 100 MHz) δ: 13.3, 56.2, 105.4, 109.1, 112.3, 114.1, 117.4, 117.5, 120.6, 122.9, 125.4, 134.2, 146.7, 151.8, 159.3, 169.2. Elemental analysis calcd (%) for $C_{16}H_{13}N_3O_3S$ (MW 327.36) C 58.71, H 4.00, N 12.84. Found C 58.80, H 4.08, N 12.79.

*(E)-5-hydroxy-3-((6-methoxy-2-methylimidazo[2,1-b]thiazol-5-yl)methylene)-6-methylindolin-2-one (**32**).* Red solid; 29% yield; mp 175-177 °C. IR cm^{-1} 1670, 1603, 1532, 1017. ^{1}H NMR (DMSO-d_6, 400 MHz) δ: 2.11 (3H, s, CH_3), 2.42 (3H, s, CH_3), 4.02 (3H, s, O-CH_3), 6.53 (1H, s, ind), 6.56 (1H, s, ind), 7.35 (1H, s, CH), 7.77 (1H, s, th), 8.73 (1H, s, OH) 10.04 (1H, s, NH). Elemental analysis calcd (%) for $C_{17}H_{15}N_3O_3S$ (MW 341.39) C 59.81, H 4.43, N 12.31. Found C 59.88, H 4.48, N 12.29.

*(E)-4,7-dimethoxy-3-((6-methoxy-2-methylimidazo[2,1-b]thiazol-5-yl)methylene)indolin-2-one (**33**).* Brown solid; 56% yield; mp 193-195 °C. IR cm^{-1} 1690, 1585, 1261, 1003. ^{1}H NMR (DMSO-d_6, 400 MHz) δ: 2.43 (3H, s, CH_3), 3.78 (3H, s, O-CH_3), 3.85 (3H, s, O-CH_3), 4.01 (3H, s, O-CH_3), 6.55 (1H, d, ind, *J*=9 Hz), 6.81 (1H, d, ind, *J*=9 Hz), 7.38 (1H, s, th), 7.81 (1H, s, CH), 10.53 (1H, s, NH). Elemental analysis calcd (%) for $C_{18}H_{17}N_3O_4S$ (MW 371.41) C 58.21, H 4.61, N 11.31. Found C 58.32, H 4.67, N 11.39.

*(E)-4,5,6-trimethoxy-3-((6-methoxy-2-methylimidazo[2,1-b]thiazol-5-yl)methylene)indolin-2-one (**34**).* Red solid; 30% yield; mp 270-272 °C. IR cm^{-1} 1680, 1578, 1291, 1091. ^{1}H NMR (DMSO-d_6, 400 MHz) δ: 2.44 (3H, s, CH_3), 3.71 (3H, s, O-CH_3), 3.81 (3H, s, O-CH_3), 3.91 (3H, s, O-CH_3), 4.01 (3H, s, O-CH_3), 6.32 (1H, s, ind), 7.42 (1H, s, th), 7.64 (1H, s, CH), 10.36 (1H, s, NH).). ^{13}C NMR (DMSO-d_6, 100 MHz) δ: 13.3, 56.1, 56.5, 60.0, 60.8, 90.7, 106.5, 108.7, 116.6, 117.5, 121.7, 122.2, 135.9, 136.5, 147.1, 148.5, 153.4, 161.2, 167.4. (Elemental analysis calcd (%) for $C_{19}H_{19}N_3O_5S$ (MW 401.44) C 56.85, H 4.77, N 10.47. Found C 56.93, H 4.89, N 10.43.

*(E)-5-chloro-3-((6-methoxy-2-methylimidazo[2,1-b]thiazol-5-yl)methylene)indolin-2-one (**35**).* Yellow solid; 47% yield; mp 270-275 °C. IR cm^{-1} 1690, 1609, 1153, 717. ^{1}H NMR (DMSO-d_6,

400 MHz) δ: 2.44 (3H, s, CH_3), 4.06 (3H, s, O-CH_3), 6.83 (1H, d, ind-6/7, *J*=8.0 Hz), 6.99 (1H, s, ind), 7.17 (1H, d, ind-6/7, *J*=8.0 Hz), 7.59 (1H, s, CH), 7.98 (1H, s, th), 10.57 (1H, s, NH). Elemental analysis calcd (%) for $C_{16}H_{12}ClN_3O_2S$ (MW 345.80) C 55.57, H 3.50, N 12.15. Found C 55.62, H 3.56, N 12.12.

4,7-Dichloro-3-((6-methoxy-2-methylimidazo[2,1-b]thiazol-5-yl)methylene)indolin-2-one (***36***). Yellow solid; 52% yield; *E/Z* 68/32; mp 280-283 °C. IR cm^{-1} 1696, 1588, 1153, 1081. ^1H NMR (DMSO-d_6, 400 MHz) δ: 2.50 (3H, s, CH_3), 4.06 (3H, s, O-CH_3), 7.01 (1H, d, ind-5/6, *J*=9.2 Hz), 7.21 (1H, d, ind-5/6, *J*=9.2 Hz), 7.46 (1H, s, CH), 8.21 (1H, s, th), 11.13 (1H, s, NH). Elemental analysis calcd (%) for $C_{16}H_{11}Cl_2N_3O_2S$ (MW 380.24) C 50.54, H 2.92, N 11.05. Found C 50.62, H 2.95, N 10.99.

(E)-3-((6-methoxy-2-methylimidazo[2,1-b]thiazol-5-yl)methylene)-1,3-dihydro-2H-benzo[g]indol-2-one (***37***). Dark red solid; 72% yield; mp 279-280 °C. IR cm^{-1} 1675, 1598, 1514, 1174. ^1H NMR (DMSO-d_6, 400 MHz) δ: 2.43 (3H, s, CH_3), 4.01 (3H, s, O-CH_3), 7.27 (1H, d, ind, *J*=8.4 Hz), 7.48 (3H, m), 7.57 (1H, s, CH), 7.87 (2H, m), 8.12 (1H, m), 11.23 (1H, s, NH).). ^{13}C NMR (DMSO-d_6, 100 MHz) δ: 13.3, 56.2, 105.9, 116.9, 117.6, 117.9, 118.9, 119.7, 121.1, 122.2, 122.3, 125.5, 126.1, 128.2, 132.7, 138.1, 147.1, 159.7, 171.1. Elemental analysis calcd (%) for $C_{20}H_{15}N_3O_2S$ (MW 361.42) C 66.47, H 4.18, N 11.63. Found C 66.64, H 4.23, N 11.73.

(E)-3-((6-methyl-[5,6'-biimidazo[2,1-b]thiazol]-5'-yl)methylene)indolin-2-one (***38***). Red orange solid; 74% yield; mp 238-240 °C. IR cm^{-1} 3417, 1696, 1600, 1206. ^1H NMR (DMSO-d_6, 400 MHz) δ: 2.02 (3H, s, CH_3), 6.45 (1H, d, ind, *J*=7.2 Hz), 6.52 (1H, t, ind, *J*=7.2, 0.8 Hz), 6.78 (1H, d, ind, *J*=7.2 Hz), 7.09 (1H, t, ind, *J*=7.2, 0.8 Hz), 7.26 (1H, d, th, *J*=4.4 Hz), 7.48 (1H, d, th, *J*=4.4 Hz), 7.57 (1H, s, CH), 7.87 (1H, d, th, *J*=4.4 Hz), 7.88 (1H, d, th, *J*=4.4 Hz), 10.54 (1H,

s, NH).). ^{13}C NMR (DMSO-d_6, 100 MHz) δ: 15.0, 109.4, 112.5, 114.6, 117.1, 118.8, 118.9, 119.6, 120.3, 120.4, 120.6, 123.1, 125.2, 129.5, 138.8, 142.4, 142.7. Elemental analysis calcd (%) for $C_{20}H_{13}N_5OS_2$ (MW 403.48) C 59.54, H 3.25, N 17.36. Found C 59.63, H 3.19, N 17.43.

*5-Methoxy-3-((6-methyl-[5,6'-biimidazo[2,1-b]thiazol]-5'-yl)methylene)indolin-2-one (**39**).* Red solid; 15% yield; *E/Z* 90/10; mp 200-210 °C. IR cm^{-1} 3114, 1690, 1608, 1204. ^{1}H NMR (DMSO-d_6, 400 MHz) δ: 2.14 (3H, s, CH_3), 3.71 (3H, s, O-CH_3), 6.72 (2H, m, ind), 7.30 (1H, d, th, *J*=4.5 Hz), 7.38 (1H, d, th, *J*=4.5 Hz), 7.43 (1H, m, ind), 7.57 (1H, s, CH), 7.65 (1H, d, th, *J*=4.2 Hz), 7.99 (1H, d, th, *J*=4.2 Hz), 10.40 (1H, s, NH). Elemental analysis calcd (%) for $C_{21}H_{15}N_5O_2S_2$ (MW 433.50) C 58.18, H 3.49, N 16.16. Found C 58.24, H 3.52, N 16.20.

*5-Chloro-3-((6-methyl-[5,6'-biimidazo[2,1-b]thiazol]-5'-yl)methylene)indolin-2-one (**40**).* Red orange solid; 20% yield; *E/Z* 77/23; mp 200-205 °C. IR cm^{-1} 1706, 1614, 1204, 897. ^{1}H NMR (DMSO-d_6, 400 MHz) δ: 1.95 (3H, s, CH_3), 6.28 (1H, d, ind-4, *J*=2.1 Hz), 6.73 (1H, d, ind-7, *J*=8.0 Hz), 7.07 (1H, dd, ind-6, *J*=8.0, 2.1 Hz), 7.25 (1H, d, th, *J*=4.4 Hz), 7.51 (1H, d, th, *J*=4.4 Hz), 7.82 (1H, s, CH), 7.86 (1H, d, th, *J*=4.4 Hz), 8.18 (1H, d, th, *J*=4.4 Hz), 10.64 (1H, s, NH). Elemental analysis calcd (%) for $C_{20}H_{12}ClN_5OS_2$ (MW 437.92) C 54.85, H 2.76, N 15.99. Found C 54.89, H 2.77, N 16.03.

*6-Chloro-3-((6-methyl-[5,6'-biimidazo[2,1-b]thiazol]-5'-yl)methylene)indolin-2-one (**41**).* Yellow orange solid; 21% yield; *E/Z* 68/32; mp 180-190 °C. IR cm^{-1} 1706, 1619, 1153, 1071. ^{1}H NMR (DMSO-d_6, 400 MHz) δ: 2.03 (3H, s, CH_3), 6.42 (1H, d, ind-4, *J*=8.2 Hz), 6.52 (1H, dd, ind-5, *J*=8.2, 2.0 Hz), 6.79 (1H, d, ind-7, *J*=2.0 Hz), 7.26 (1H, d, th, *J*=4.5 Hz), 7.50 (1H, d, th, *J*=4.5 Hz), 7.64 (1H, s, CH), 7.83 (1H, d, th, *J*=4.5 Hz), 7.95 (1H, d, th, *J*=4.5 Hz), 10.71 (1H, s,

NH). Elemental analysis calcd (%) for $C_{20}H_{12}ClN_5OS_2$ (MW 437.92) C 54.85, H 2.76, N 15.99. Found C 5489, H 2.81, N 16.03.

*3-((6-Methyl-[5,6'-biimidazo[2,1-b]thiazol]-5'-yl)methylene)-1,3-dihydro-2H-benzo[g]indol-2-one (**42**)*. Orange solid; 20% yield; *E/Z* 65/35; mp 240-245 °C. IR cm^{-1} 1685, 1609, 1250, 810. ^1H NMR (DMSO-d_6, 400 MHz) δ: 2.02 (3H, s, CH_3), 6.69 (1H, d, ind, *J*=8.4 Hz), 7.02 (1H, d, ind, *J*=8.4 Hz), 7.28 (1H, d, th, *J*=4.4 Hz), 7.48 (1H, d, th, *J*=4.0 Hz), 7.50 (2H, m, ind), 7.65 (1H, s, CH), 7, 75 (1H, m, ind), 7.94 (1H, d, th, *J*=4.4 Hz), 7.98 (1H, d, th, *J*=4.0 Hz), 8.08 (1H, d, ind, *J*=8.0 Hz), 11.33 (1H, s, NH). Elemental analysis calcd (%) for $C_{24}H_{15}N_5OS_2$ (MW 453.54) C 63.56, H 3.33, N 15.44. Found C 63.58, H 3.41, N 15.51.

*(E)-3-((2',6-dimethyl-[5,6'-biimidazo[2,1-b]thiazol]-5'-yl)methylene)-1-methylindolin-2-one (**43**)*. Yellow orange solid; 32% yield; mp 194-196 °C. IR cm^{-1} 1698, 1610, 1163, 1086. ^1H NMR (DMSO-d_6, 400 MHz) δ: 1.99 (3H, s, CH_3), 2.44 (3H, s, CH_3), 3.21 (3H, s, N-CH_3), 6.51 (1H, d, ind-4/7, *J*=7.6 Hz), 6.60 (1H, t, ind-5/6, *J*=7.6 Hz), 6.96 (1H, d, ind-4/7, *J*=7.6 Hz), 7.18 (1H, t, ind-5/6, *J*=7.6 Hz), 7.25 (1H, d, th, *J*=4.4 Hz) 7.60 (1H, s, CH), 7.68 (1H, s, th), 7.87 (1H, d, th, *J*=4.4 Hz). Elemental analysis calcd (%) for $C_{22}H_{17}N_5OS_2$ (MW 431.53) C 61.23, H 3.97, N 16.23. Found C 61.31, H 4.01, N 16.33.

*3-((2',6-Dimethyl-[5,6'-biimidazo[2,1-b]thiazol]-5'-yl)methylene)-1-phenylindolin-2-one (**44**).* Orange solid; 37% yield; *E/Z* 79/21; mp 150-155 °C. IR cm^{-1} 1704, 1598, 1183, 1091. ^1H NMR (DMSO-d_6, 400 MHz) δ: 2.09 (3H, s, CH_3), 2.47 (3H, q, CH_3, *J*=1.6 Hz), 6.60 (1H, d, ind, *J*=7.6 Hz), 6.65 (1H, t, ind, *J*=7.6 Hz), 6.70 (1H, d, ind, *J*=7.6 Hz), 7.12 (1H, t, ind, *J*=7.6 Hz), 7.27 (1H, d, th, *J*=4.4 Hz), 7.49 (3H, m, ar), 7.59 (2H, m, ar), 7.73 (1H, s, CH), 7.80 (1H, d, th, *J*=1.6

Hz), 7.85 (1H, d, th, *J*=4.4 Hz). Elemental analysis calcd (%) for $C_{27}H_{19}N_5OS_2$ (MW 493.60) C 65.70, H 3.88, N 14.19. Found C 65.75, H 3.91, N 14.22.

3-((2',6-Dimethyl-[5,6'-biimidazo[2,1-b]thiazol]-5'-yl)methylene)-5-methoxyindolin-2-one ***(45)***. Red orange solid; 43% yield; *E/Z* 74/26; mp 195-197 °C. IR cm^{-1} 1701, 1296, 1189, 1030. ^1H NMR (DMSO-d_6, 400 MHz) δ: 1.95 (3H, s, CH_3), 2.47 (3H, q, CH_3, *J*=1.2 Hz), 3.30 (3H, s, OCH_3), 6.04 (1H, s, ind), 6.70 (2H, s, ind), 7.25 (1H, d, th, *J*=4.4 Hz), 7.55 (1H, s, CH), 7.76 (1H, d, th, *J*=1.2 Hz), 7.94 (1H, d, th, *J*=4.4 Hz), 10.37 (1H, s, NH). Elemental analysis calcd (%) for $C_{22}H_{17}N_5O_2S_2$ (MW 447.53) C 59.04, H 3.83, N 15.65. Found C 58.99, H 3.85, N 15.67.

(E)-3-((2',6-dimethyl-[5,6'-biimidazo[2,1-b]thiazol]-5'-yl)methylene)-5-methoxy-1-methylindolin-2-one ***(46)***. Red solid; 46% yield; mp 255-259 °C. IR cm^{-1} 1693, 1629, 1273, 974. ^1H NMR (DMSO-d_6, 400 MHz) δ: 1.93 (3H, s, CH_3), 2.46 (3H, s, CH_3), 3.19 (3H, s, N-CH_3), 3.42 (3H, s, O-CH_3), 6.09 (1H, d, ind-4, *J*=2.3 Hz), 6.79 (1H, dd, ind-6, *J*=8.5, 2.3 Hz), 6.89 (1H, d, ind-7, *J*=8.5 Hz), 7.26 (1H, d, th, *J*=4.4 Hz), 7.63 (1H, s, CH), 7.75 (1H, s, th), 7.95 (1H, d, th, *J*=4.4 Hz). Elemental analysis calcd (%) for $C_{23}H_{19}N_5O_2S_2$ (MW 461.56) C 59.85, H 4.15, N 15.17. Found C 59.91, H 4.21, N 15.20.

(E)-3-((2',6-dimethyl-[5,6'-biimidazo[2,1-b]thiazol]-5'-yl)methylene)-5-hydroxyindolin-2-one ***(47)***. Red solid; 38% yield; mp >315 °C. IR cm^{-1} 3500, 1680, 1603, 1204. ^1H NMR (DMSO-d_6, 400 MHz) δ: 2.05 (3H, s, CH_3), 2.45 (3H, q, CH_3, *J*=1.4 Hz), 6.02 (1H, d, ind-4, *J*=2.0 Hz), 6.55 (1H, dd, ind-6, *J*=8.5, 2.0 Hz), 6.62 (1H, d, ind-7, *J*=8.5 Hz), 7.24 (1H, d, th, *J*=4.5 Hz), 7.38 (1H, s, CH), 7.54 (1H, d, th, *J*=1.4 Hz), 7.87 (1H, d, th, *J*=4.5), 8.74 (1H, s, OH), 10.28 (1H, s, NH). Elemental analysis calcd (%) for $C_{21}H_{15}N_5O_2S_2$ (MW 433.50) C 58.18, H 3.49, N 16.16. Found C 58.22, H 3.52, N 16.20.

*(E)-3-((2',6-dimethyl-[5,6'-biimidazo[2,1-b]thiazol]-5'-yl)methylene)-5-fluoroindolin-2-one (**48**).* Red solid; 35% yield; mp 255-258 °C. IR cm^{-1} 3560, 1689, 1602, 1250. ^1H NMR (DMSO-d_6, 400 MHz) δ: 1.99 (3H, s, CH_3), 2.47 (3H, q, CH_3, *J*=1.6 Hz), 6.12 (1H, dd, ind-4, *J*=9.0, 2.6 Hz), 6.70 (1H, dd, ind-7, *J*=8.6, 4.4 Hz), 6.88 (1H, td, ind-6, *J*=9.0, 2.6 Hz), 7.23 (1H, d, th, *J*=4.4 Hz), 7.68 (1H, s, CH), 7.79 (1H, d, th, *J*=4.4 Hz), 7.90 (1H, d, th, *J*=1.6 Hz), 10.53 (1H, s, NH). Elemental analysis calcd (%) for $C_{21}H_{14}FN_5OS_2$ (MW 435.50) C 57.92, H 3.24, N 16.08. Found C 56.89, H 3.30, N 16.13.

*5-Chloro-3-((2',6-dimethyl-[5,6'-biimidazo[2,1-b]thiazol]-5'-yl)methylene)indolin-2-one (**49**).* Dark red solid; 18% yield; *E/Z* 78/22; mp 200-202 °C. IR cm^{-1} 1702, 1610, 1204, 1102. ^1H NMR (DMSO-d_6, 400 MHz) δ: 1.93 (3H, s, CH_3), 2.48 (3H, q, CH_3, *J*=1.6 Hz), 6.26 (1H, d, ind, *J*=2.2 Hz), 6.73 (1H, d, ind, *J*=8.4 Hz), 7.06 (1H, dd, ind, *J*=8.4, 2.2 Hz), 7.24 (1H, d, th, *J*=4.4 Hz), 7.76 (1H, s, CH), 7.85 (1H, d, th, *J*=4.4 Hz), 8.00 (1H, d, th, *J*=1.6 Hz), 10.62 (1H, s, NH). Elemental analysis calcd (%) for $C_{21}H_{14}ClN_5OS_2$ (MW 451.95) C 55.81, H 3.12, N 15.50. Found C 55.83, H 3.15, N 15.54.

*(E)-3-((2',6-dimethyl-[5,6'-biimidazo[2,1-b]thiazol]-5'-yl)methylene)-4-fluoroindolin-2-one (**50**).* Red solid; 43% yield; mp 268-270 °C. IR cm^{-1} 3575, 1688, 1603, 1250. ^1H NMR (DMSO-d_6, 400 MHz) δ: 2.01 (3H, s, CH_3), 2.45 (3H, q, CH_3, *J*=1.2 Hz), 6.28 (1H, td, ind-6, *J*=8.4, 2.4 Hz), 6.44 (1H, dd, ind-5, *J*=8.4, 5.6 Hz), 6.59 (1H, dd, ind-7, *J*=9.4, 2.4 Hz), 7.24 (1H, d, th, *J*=4.4 Hz), 7.53 (1H, s, CH), 7.75 (1H, d, th, *J*=1.2 Hz), 7.81 (1H, d, th, *J*=4.4 Hz), 10.63 (1H, broad, NH). Elemental analysis calcd (%) for $C_{21}H_{14}FN_5OS_2$ (MW 435.50) C 57.92, H 3.24, N 16.08, Found C 57.89, H 3.26, N 16.11.

(E)-4-chloro-3-((2',6-dimethyl-[5,6'-biimidazo[2,1-b]thiazol]-5'-yl)methylene)indolin-2-one ***(51)***. Red solid; 44% yield; mp 217-220 °C. IR cm^{-1} 1701, 1680, 1578, 881. ^{1}H NMR (DMSO-d_6, 400 MHz) δ: 2.19 (3H, s, CH_3), 2.65 (3H, s, CH_3), 6.91 (1H, d, ind-5/7, *J*=8 Hz), 7.04 (1H, d, ind-5/7, *J*=8.0 Hz),7.25 (1H, t, ind-6, *J*=8.0 Hz), 7.31 (1H, d, th, *J*=4.4 Hz), 7.50 (1H, s, th), 7.93 (1H, s, CH), 8.03 (1H, d, th, *J*=4.4 Hz), 10.90 (1H, s, NH). Elemental analysis calcd (%) for $C_{21}H_{14}ClN_5OS_2$ (MW 451.95) C 55.81, H 3.12, N 15.50. Found 55.79, H 3.10, N 15.48.

(E)-6-chloro-3-((2',6-dimethyl-[5,6'-biimidazo[2,1-b]thiazol]-5'-yl)methylene)indolin-2-one ***(52)***. Red solid; 33% yield; mp 279-281 °C. IR cm^{-1} 1696, 1609, 1071, 979. ^{1}H NMR (DMSO-d_6, 400 MHz) δ: 2.01 (3H, s, CH_3), 2.46 (3H, s, CH_3), 6.41 (1H, d, ind-4, *J*=8.3 Hz), 6.52 (1H, dd, ind-5, *J*=8.3, 1.8 Hz), 6.78 (1H, d, ind-7, *J*=1.8 Hz), 7.25 (1H, d, th, *J*=4.4 Hz), 7.59 (1H, s, CH), 7.77 (1H, s, th), 7.81 (1H, d, th, *J*=4.4 Hz), 10.69 (1H, s, NH). Elemental analysis calcd (%) for $C_{21}H_{14}ClN_5OS_2$ (MW 451.95) C 55.81, H 3.12, N 15.50. Found C 55.79, H 3.10, N 15.47.

*4.1.2. Synthesis of 6-methoxy-2-methylimidazo[2,1-b]thiazole-5-carbaldehyde (**1c**)*

6-Chloro-2-methylimidazo[2,1-*b*]thiazole-5-carbaldehyde (10 mmol) was dissolved in methanol (100 mL) and treated with CH_3ONa (50 mmol). The reaction mixture was kept for 3 h at room temperature and under reflux for 5 h. After cooling, methanol was evaporated under reduced pressure, and the residue was added to water. The resulting precipitate was collected by filtration and crystallized from methanol.

Orange solid; 65% yield; mp 119-121 °C. IR (cm^{-1}): 1639, 1547, 1107, 1004. ^{1}H NMR (DMSO-d_6, 400 MHz) δ: 2.45 (3H, d, CH_3, *J*=1.5 Hz), 4.02 (3H, s, CH_3), 8.03 (1H, q, th, *J*=1.5 Hz), 9.46 (1H, s, CH). Anal. Calcd for $C_8H_8N_2O_2S$ (MW 196.22) C 48.97, H 4.11, N 14.28. Found C 49.01, H 4.10, N 14.37.

*4.1.3. Synthesis of imidazo[2,1-b]thiazoles **57d,e***

2-Aminothiazole or 5-methylthiazol-2-amine **54d,e** (20 mmol) was dissolved in 100 mL of acetone and treated with one equivalent of 2-bromo-1-(6-methylimidazo[2,1-*b*]thiazol-5-yl)ethan-1-one **55**. The reaction mixture was refluxed for 9-10 h (reaction followed by TLC), and the resulting salt (**56d,e**) was separated by filtration and used without further purification ($\nu_{C=O}$ absorption was confirmed around 1700 cm^{-1}) in the subsequent step. It was refluxed for 1 h with 200 mL of 2 N HCl, and, before complete cooling, the solution was cautiously basified by dropwise addition of 15% NH_4OH. The resulting base was collected by filtration and crystallized from acetone/petroleum ether.

*6-Methyl-5,6'-biimidazo[2,1-b]thiazole (**57d**).* Red solid; yield 50%; mp 169-171 °C; IR (cm^{-1}): 1595, 1020, 861, 723; ^{1}H NMR (DMSO-d_6, 400 MHz) δ: 2.41 (3H, s, CH3), 7.25 (1H, d, th, *J*=4.4 Hz), 7.31 (1H, d, th, *J*=4.4 Hz), 7.95 (1H, d, th, *J*=4.4 Hz), 8.02 (1H, s, im), 8.29 (1H, d, th, *J*=4.4 Hz). Anal. Calcd for $C_{11}H_8N_4S_2$ (MW 260.33): C, 50.75; H, 3.10; N, 21.52. Found: C, 50.78; H, 3.15; N, 21.50.

*2',6-Dimethyl-5,6'-biimidazo[2,1-b]thiazole (**57e**).* Red solid; yield 30%; mp 173-175°C; IR (cm^{-1}): 1598, 1189, 835, 799; ^{1}H NMR (DMSO-d_6, 400 MHz) δ: 2.40 (6H, s, 2xCH_3), 7.23 (1H, d, th, *J*=4.4 Hz), 7.70 (1H, s, th), 7.92 (1H, s, im), 8.28 (1H, d, th, *J*=4.4 Hz). Anal. Calcd for $C_{12}H_{10}N_4S_2$ (MW 274.36): C, 52.53; H, 3.67; N, 20.42. Found: C, 52.49; H, 3.71; N, 20.38.

*4.1.4. Synthesis of aldehydes **1d**,**e***

The Vilsmeier reagent was prepared at 0-5 °C by dropping $POCl_3$ (54 mmol) into a stirred solution of DMF (65 mmol) in $CHCl_3$ (5 mL). The appropriate condensed imidazole **57d**,**e** (5 mmol) was suspended in $CHCl_3$ (20 mL). The mixture thus obtained was dropped into the

Vilsmeier reagent while maintaining stirring and cooling. The reaction mixture was kept for 3 h at room temperature and under reflux for 4 h. Chloroform was removed under reduced pressure and the resulting oil was poured onto ice. The solution was basified by addition of NH_4OH, and the crude aldehydes **1d**,**e** were crystallized from ethanol.

*6-Methyl-[5,6'-biimidazo[2,1-b]thiazole]-5'-carbaldehyde (**1d**).* Red solid; yield 80%; mp 240-242°C; IR (cm^{-1}): 1658, 1149, 1020, 721; ^{1}H NMR (DMSO-d_6, 400 MHz) δ: 2.41 (3H, s, CH_3), 7.31 (1H, d, th, *J*=4.4 Hz), 7.61 (1H, d, th, *J*=4.4 Hz), 7.97 (1H, d, th, *J*=4.4 Hz), 8.41 (1H, d, th, *J*=4.4 Hz), 9.69 (1H, s, CHO). Anal. Calcd for $C_{12}H_8N_4OS_2$ (MW 288.34): C, 49.99; H, 2.80; N, 19.43. Found: C, 49.78; H, 2.85; N, 19.48.

*2',6-Dimethyl-[5,6'-biimidazo[2,1-b]thiazole]-5'-carbaldehyde (**1e**).* Red solid; yield 75%; mp 282-284 °C; IR (cm^{-1}): 1643, 1152, 1020, 723; ^{1}H NMR (DMSO-d_6, 400 MHz) δ: 2.55 (6H, s, 2xCH_3), 6.86 (1H, d, th, *J*=4.4 Hz), 7.87 (1H, d, th, *J*=4.4 Hz), 8.11 (1H, s, th), 8.71 (1H, s, CHO). Anal. Calcd for $C_{13}H_{10}N_4OS_2$ (MW 302.37): C, 51.64; H, 3.33; N, 18.53; O, 5.29; S, 21.21. Found: C, 51.60; H, 3.35; N, 18.53.

4.2. Biology

4.2.1. Cell-Based Screening Assay

The NCI screening process [38] occurs in two stages, beginning with the evaluation of all compounds against the 60 cell lines at 10^{-5} M. Compounds exhibiting significant growth inhibition are subsequently evaluated against the 60 cell lines at five concentration levels according to standard procedures (http://dtp.nci.nih.gov/branches/btb/ivclsp.html). In both cases, the exposure time is 48 h.

4.2.2. Cell growth conditions and antiproliferative assay

PBL from healthy donors were obtained by separation on a Lymphoprep (Fresenius KABI Norge AS) gradient. After extensive washing, cells were resuspended (1.0 x 10^6 cells/mL) in RPMI-1640 with 10% fetal bovine serum and incubated overnight.

For cytotoxicity evaluations in proliferating PBL cultures, non-adherent cells were resuspended at 5 x 10^5 cells/mL in growth medium, containing 2.5 μg/mL PHA (Irvine Scientific). Different concentrations of the test compounds were added, and viability was determined 72 h later by the MTT test. For cytotoxicity evaluations in resting PBL cultures, non-adherent cells were resuspended (5 x 10^5 cells/mL) and treated for 72 h with the test compounds. Cell viability was assayed by the (3-(4,5-dimethylthiazol-2-yl)-2,5-diphenyltetrazolium bromide test as previously described [32,33].

4.2.3. Effects on tubulin polymerization and on colchicine binding to tubulin

To evaluate the effect of the compounds on tubulin assembly *in vitro* [25], varying concentrations of compounds were preincubated with 10 μM bovine brain tubulin in glutamate buffer at 30 °C and then cooled to 0 °C. After addition of 0.4 mM GTP (final concentration), the mixtures were transferred to 0 °C cuvettes in a recording spectrophotometer equipped with an electronic temperature controller and warmed to 30 °C. Tubulin assembly was followed turbidimetrically at 350 nm. The IC_{50} was defined as the compound concentration that inhibited the extent of assembly by 50% after a 20 min incubation. The ability of the test compounds to inhibit colchicine binding to tubulin was measured as described [39], except that the reaction mixtures contained 1 μM tubulin, 5 μM [^{3}H]colchicine and 5 or 50 μM test compound.

4.2.4. Flow cytometric analysis of cell cycle distribution

5×10^5 HeLa cells were treated with different concentrations of the test compounds for 24 h. After the incubation period, the cells were collected, centrifuged, and fixed with ice-cold ethanol (70%). The cells were then treated with lysis buffer containing RNase A and 0.1% Triton X-100 and then stained with PI. Samples were analyzed on a Cytomic FC500 flow cytometer (Beckman Coulter). DNA histograms were analyzed using MultiCycle for Windows (Phoenix Flow Systems).

4.2.5. Mitotic index

K562 human leukemia cells were grown in RPMI 1640 medium supplemented with 5% fetal bovine serum for 16 h in a 5% CO_2, humidified atmosphere at 37 °C. Cells were harvested by centrifugation, smeared onto a glass slide, fixed with ethanol, stained with Giemsa, and the proportion of cells with condensed chromosomes was determined. Without compounds the mitotic index was 3%.

4.2.6. Apoptosis assay

Cell death was determined by flow cytometry of cells double stained with annexin V/FITC and PI. The Coulter Cytomics FC500 (Beckman Coulter) was used to measure the surface exposure of phosphatidyl serine on apoptotic cells according to the manufacturer's instructions (Annexin-V Fluos, Roche Diagnostics).

4.2.6. Western blot analysis

HeLa cells were incubated in the presence of the test compounds and, after different times, were collected, centrifuged, and washed two times with ice-cold phosphate-buffered saline (PBS). The pellet was then resuspended in lysis buffer. After the cells were lysed on ice for 30 min, lysates were centrifuged at 15000 x g at 4 °C for 10 min. The protein concentration in the supernatant was determined using the BCA protein assay reagents (Pierce, Italy). Equal

amounts of protein (10 μg) were resolved using sodium dodecyl sulfate-polyacrylamide gel electrophoresis (Criterion Precast, BioRad, Italy) and transferred to a PVDF Hybond-P membrane (GE Healthcare). Membranes were blocked with a bovine serum albumin solution (5% in Tween PBS 1X), the membranes being gently rotated overnight at 4 °C. Membranes were then incubated with primary antibodies against Bcl-2, Mcl-1, PARP, cdc25c, cyclin B, p-cdc2^{Tyr15}, Cleaved caspase-9 (Asp330), Cleaved caspase-3 (Asp175) (all from Cell Signaling), or β-actin (Sigma-Aldrich) for 2 h at room temperature. Membranes were next incubated with peroxidase labeled secondary antibodies for 60 min. All membranes were visualized using ECL Select (GE Healthcare), and images were acquired using an Uvitec-Alliance imaging system (Uvitec, Cambridge, UK). To ensure equal protein loading, each membrane was stripped and reprobed with anti-β-actin antibody. Densitometric analysis of western blot was performed by Image J software and the results were normalized to β-actin and represented as fold change respect to untreated controls.

4.2.7. In vivo animal studies

Animal experiments were approved by our local animal ethics committee (OPBA, Organismo Preposto al Benessere degli Animali, Università degli Studi di Brescia, Italy) and were executed in accordance with national guidelines and regulations. Procedures involving animals and their care conformed with institutional guidelines that comply with national and international laws and policies (EEC Council Directive 86/609, OJ L 358, 12 December 1987) and with "ARRIVE" guidelines (Animals in Research Reporting *In Vivo* Experiments). Six weeks old C57BL/6 mice (Envigo) were injected subcutaneously into the dorsolateral flank with $2.5x10^5$ BL6-B16 murine melanoma cells in 200 μL-total volume of PBS. Six weeks old C57BL/6 female mice (Envigo) were injected subcutaneously into the dorsolateral flank with $2.5x10^5$ E0771 murine breast cancer cells in 200 μL of PBS. When tumors were palpable, animals were treated intraperitoneally every other day with different doses of test compounds

dissolved in 50 µL of DMSO. Tumors were measured in two dimensions, and tumor volume was calculated according to the formula $V=(D \times d^2)/2$, where D and d are the major and minor perpendicular tumor diameters, respectively.

Statistical analysis.

Graphs and statistical analyses were performed using GraphPad Prism 7.05 software (GraphPad, La Jolla, CA). All data in histograms and plots represent the mean of at least three independent experiments ±standard error of the mean (SEM). Statistical significance was analysed using Student t test or ANOVA (one- or two-way) depending on the type of data. For multiple test comparison, Dunnett's test were applied. Asterisks indicate a significant difference between the treated and the control group, unless otherwise specified; *$p < 0.05$, **$p < 0.01$, ***$p < 0.001$, ****$p < 0.0001$.

For tumor volume evaluation data were analyzed with a 2-way analysis of variance, and individual group comparisons were evaluated by the Bonferroni correction.

Disclaimer

The content of this paper is solely the responsibility of the authors and does not necessarily reflect the official views of the National Institutes of Health.

Author Informations

*To whom correspondence should be addressed: (R.M.): Phone: 39-(0)51-2099712. Fax: 39-(0)51-2099734. E-mail: rita.morigi@unibo.it. (G.V.): Phone: 39-(0)49-8215485. Fax: 39-(0)49-8211462. E-mail:giampietro.viola1@unipd.it.

Notes. The authors declare no competing financial interest.

Acknowledgement

This work was supported in part by a grant from the University of Bologna, Italy (RFO). We are grateful to the National Cancer Institute (Bethesda, MD) for the anticancer tests.

Abbreviations. CA-4**,** combretastatin A-4; CA-4P, combretastatin 4-A phosphate; PI, propidium iodide; PS, phosphatidylserine; PARP, polyADP-ribose polymerase; PBL, peripheral blood lymphocytes; PHA, phytohemaglutinin; FITC, fluorescein isothiocyanate; BSA, bovine serum albumin; PBS, phosphate-buffered saline; SDS-PAGE, sodium dodecyl sulfate polyacrylamide gel electrophoresis;

References

[1]. a) N.G. Vindya, N. Sharma, M. Yadav, K.R. Ethiraj. Tubulins-the target for anticancer therapy. Curr. Top. Med. Chem. 15 (2015) 73-82. b) C. Dumontet, M.A. Jordan. Microtubule-binding agents: a dynamic field of cancer therapeutics. Nat. Rev. Drug. Discov. 9 (2010) 790-803.

[2] R.A. Stanton, K.M. Gernert, J.H. Nettles, R. Aneja. Drugs that target dynamic microtubules: a new molecular perspective. Med. Res. Rev. 31 (2011) 443-481.

[3] Y. Lu, J. Chen, M. Xiao, W. Li, D.D. Miller. An overview of tubulin inhibitors that interact with the colchicine binding site. Pharm. Res. 29 (2012) 2943-2971.

[4] A. Andreani, M. Granaiola, A. Locatelli, R. Morigi, M. Rambaldi, L. Varoli, N. Calonghi, C. Cappadone, G. Farruggia, C. Stefanelli, L. Masotti, T.L. Nguyen, E. Hamel, R.H. Shoemaker. Substituted 3-(5-imidazo[2,1-*b*]thiazolylmethylene)-2-indolinones and analogues: synthesis, cytotoxic activity, and study of the mechanism of action. J. Med. Chem. 55 (2012) 2078-2088.

[5] A. Andreani, S. Burnelli, M. Granaiola, A. Leoni, A. Locatelli, R. Morigi, M. Rambaldi, L. Varoli, N. Calonghi, C. Cappadone, M. Voltattorni, M. Zini, C. Stefanelli, L. Masotti, R.H. Shoemaker. Antitumor activity of new substituted 3-(5-imidazo[2,1*b*]thiazolylmethylene)-2-

indolinones and 3-(5-imidazo[2,1-*b*]thiadiazolylmethylene)-2-indolinones: selectivity against colon tumor cells and effect on cell cycle-related events. J. Med. Chem. 51 (2008) 7508-7513.

[6] R. Hodges, J.S. Shannon, W.D. Jamieson, A. Taylor. Chemical and biological properties of some oxindol-3-ylidene methines. Can. J. Chem. 46 (1968) 2189-2194.

[7] C.F. Koelsch. A synthesis of ethyl quininate from m-cresol. J. Amer. Chem. Soc. 66 (1944) 2019-2020.

[8] J.C. Porter, R. Robinson, M. Wyler. Monothiophthalimide and some derivatives of oxindole. J. Chem. Soc. (1941) 620-624.

[9] R.J.S. Beer, H.F. Davenport, A. Robertson. Extensions of the synthesis of hydroxyindoles from *p*-benzoquinones. J. Chem. Soc. (1953) 1262-1264.

[10] A. Andreani, M. Rambaldi, D. Bonazzi, L. Greci, F. Andreani. Potential antitumor agents. III. Hydrazone derivatives of 5-substituted 2-chloro-3-formyl-6-methylindole. Farmaco 34 (1979) 132-138.

[11] A. Andreani, S. Bellini, S. Burnelli, M. Granaiola, A. Leoni, A. Locatelli, R. Morigi, M. Rambaldi, L. Varoli, N. Calonghi, C. Cappadone, M. Zini, C. Stefanelli, L. Masotti, R.H. Shoemaker. Substituted *E*-3-(3-indolylmethylene)-1,3-dihydroindol-2-ones with antitumor activity. In depth study of the effect on growth of breast cancer cells. J. Med. Chem. 53 (2010) 5567-5575.

[12] A. Andreani, M. Granaiola, A. Leoni, A. Locatelli, R. Morigi, M. Rambaldi, V. Garaliene. Synthesis and antitumor activity of 1,5,6-substituted 3-(2-chloro-3-indolylmethylene)1,3-dihydroindol-2-ones. J. Med. Chem. 45 (2002) 2666-2669.

[13] A. Zakrzewska, E. Kolehmainen, B. Osmialowski, R. Gawinecki. 4-Fluoroanilines: synthesis and decomposition. J. Fluorine Chem. 111 (2001) 1-10.

[14] F. Mayer, T. Oppenheimer. Über naphthyl-essigsäuren. 3. Abhandlung: 1-nitronaphthyl-2-brenztraubensäure und 1-nitronaphthyl-2-essigsäure. Chem. Ber. 51 (1918) 1239-1245.

[15] S. Sakai, N. Aimi, A. Kubo, M. Kitagawa, M. Hanasawa, K. Katano, K. Yamaguchi, J. Haginiwa. Structure of gardneramine and 18-demethylgardneramine. Chem. Pharm. Bull. 23 (1975) 2805-2817.

[16] G.N. Walker, R.T. Smith, B.N. Weaver. Synthesis of new 3-(pyridylmethylene)-, 3-(pyridylmethyl)-, 3-(piperidylmethyl)-, and 3-(β-alkylaminoethyl)-2-indolinones. The reduction of isoindogenides, nitro compounds, and pyridines in a series of 2-indolinones. J. Med. Chem. 8 (1965) 626–637.

[17] L.K. Mehta, J. Parrick, F. Payne. Preparation of 3-ethyloxindole-4,7-quinone. J. Chem. Res. (S) (1998) 190-191.

[18] B.V. Silva, N.M. Ribeiro, A.C. Pinto, M.D. Vargas, L.C. Dias. Synthesis of ferrocenyl oxindole compounds with potential anticancer activity. J. Braz. Chem. Soc. 19 (2008) 1244-1247.

[19] R.D. Clark, J.M. Muchowski, L.E. Fisher, L.A. Flippin, D.B. Repke, M. Souchet. Preparation of indoles and oxindoles from *N*-(*tert*-butoxycarbonyl)-2-alkylanilines. Synthesis 10 (1991) 871-878.

[20] A. Romeo, H. Corrodi, E. Hardegger. Umsetzungen des o-nitrophenylessigesters und des 2-chlor-6-nitro-phenyl-brenztraubensäureesters. Helv. Chim. Acta 38 (1955) 463-467.

[21] A. Andreani, M. Rambaldi, F. Andreani, R. Bossa, I. Galatulas. 6-Pyridinylimidazo[2,1-*b*]thiazoles and thiazolines as potential cardiotonic agents. Eur. J. Med. Chem. 1 (1985) 93-94.

[22] A. Andreani, M. Rambaldi, P. Carloni, L. Greci, P. Stipa. Imidazo[2,1-*b*]thiazole Carbamates and acylureas as potential insect control agents. J. Heterocyclic. Chem. 26 (1989) 525-529.

[23] H. An, B. Xi, Y. Abassi, X. Wang, X. Xu. Heterocyclic compounds and uses as anticancer agents. U.S. Patent 20090048271 A1 2009.

[24] C.M. Lin, H.H. Ho, G.R. Pettit, E. Hamel. The Antimitotic Natural Products Combretastatin A-4 and combretastatin A-2: Studies on the mechanism of their inhibition of the binding of colchicine to tubulin. Biochemistry 28 (1989) 6984-6991.

[25] E. Hamel. Evaluation of antimitotic agents by quantitative comparisons of their effects on the polymerization of purified tubulin. Cell Biochem. Biophys. 38 (2003) 1-21.

[26] B.A.A Weaver, D.W. Cleveland. Decoding the links between mitosis, cancer, and chemotherapy: the mitotic checkpoint, adaptation, and cell death. Cancer Cell 8 (2005) 7-12.

[27] P.R. Clarke, L.A. Allan. Cell-cycle control in the face of damage- a matter of life or death. Trends Cell Biol. 19 (2009) 89-98.

[28] S. Xiong, T. Mu, G. Wang, X. Jiang. Mitochondria-mediated apoptosis in mammals. *Protein* Cell 5 (2014) 737-749.

[29] A. Rovini, A. Savry, D. Braguer, M. Carré. Microtubule-targeted agents: when mitochondria become essential to chemotherapy. Biochim. Biophys. Acta-Bioenerg. 1807 (2011) 679-688.

[30] G. Viola, E. Fortunato, L. Cecconet, L. Del Giudice, F. Dall'Acqua, G. Basso. Central role of mitochondria and p53 in PUVA-induced apoptosis in human keratinocytes cell line NCTC-2544. Tox. Appl. Pharmacol. 227 (2008) 84-96.

[31] G. Mendez, C. Policarpi, C. Cenciarelli, C. Tanzarella, A. Antoccia. Role of Bim in apoptosis induced in H460 lung tumor cells by the spindle poison combretastatin-A4. Apoptosis. 16 (2011) 940-949.

[32] R. Romagnoli, P.G. Baraldi, M. Kimatrai Salvador, D. Preti, M.A. Tabrizi, A. Brancale, X-H. Fu, J. Li, R. S-Z. Zhang, E. Hamel, R. Bortolozzi, E. Porcù, G. Basso, G. Viola. Discovery and Optimisation of a Series of 2-Aryl-4-Amino-5-(3',4',5'-trimethoxybenzoyl)Thiazoles as Novel Anticancer Agents. J. Med. Chem. 55 (2012) 5433–5445.

[33] R. Romagnoli, P.G. Baraldi, C. Lopez-Cara, M. Kimatrai Salvador, D. Preti, M.A. Tabrizi, M. Bassetto, A. Brancale, E. Hamel, I. Castagliuolo, R. Bortolozzi, G. Basso, G. Viola.

Synthesis and Biological Evaluation of 2-Alkoxycarbonyl-3-Anilino Benzo[*b*]thiophenes and Thieno[2,3-*b*]Pyridines as New Potent Anticancer Agents. J. Med. Chem. 56 (2013) 2606-2618.

[34] N. Zamzami, P. Marchetti, M. Castedo, D. Decaudin, A. Macho, T. Hirsch, S.A. Susin, P.X. Petit, B. Mignotte, G. Kroemer. Sequential reduction of mitochondrial transmembrane potential and generation of reactive oxygen species in early programmed cell death. J. Exp. Med. 182 (1995) 367-377.

[35] I.E. Wertz, S. Kusam, C. Lam, T. Okamoto, W. Sandoval, D.J. Anderson, E. Helgason, J.A. Ernst, M. Eby, J. Liu, L.D. Belmont, J.S. Kaminker, K.M. O'Rourke, K. Pujara, P.B. Kohli, A.R. Johnson, M.L. Chiu, J.R. Lill, P.K. Jackson, W.J. Fairbrother, S. Seshagiri, M.J. Ludlam, K.G. Leong, E.C. Dueber, H. Maecker, D.C. Huang, V.M. Dixit. Sensitivity to antitubulin chemotherapeutics is regulated by MCL1 and FBW7. Nature 471 (2011) 110-114.

[36] P.E. Czabotar, G. Lessene, A. Strasser, J.M. Adams. Control of apoptosis by the BCL-2 protein family: implications for physiology and therapy. Nature Rev. Mol. Cell Biol. 15 (2014) 49-63.

[37] R. Ronca, E. Di Salle, A. Giacomini, D. Leali, P. Alessi, D. Coltrini, C. Ravelli, S. Matarazzo, D. Ribatti, W. Vermi, M. Presta. Long Pentraxin-3 inhibits epithelial-mesenchymal transition in melanoma cells. Mol. Cancer Ther. 12 (2013) 2760-2771.

[38] A. Monks, D. Scudiero, P. Skehan, R. Shoemaker, K. Paull, D. Vistica, C. Hose, J. Langley, P. Cronise, A. Vaigro-Wolff, M. Gray-Goodrich, H. Campbell, J. Mayo, M. Boyd. Feasibility of a high-flux anticancer drug screen using a diverse panel of cultured human tumor cell lines. J. Natl. Cancer Inst. 83 (1991) 757–766.

[39] P. Verdier-Pinard, J-Y. Lai, H-D. Yoo, J. Yu, B. Marquez, D.G. Nagle, M. Nambu, J.D. White, J.R. Falck, W.H. Gerwick, B.W. Day, E. Hamel. Structure-activity analysis of the interaction of curacin A, the potent colchicine site antimitotic agent, with tubulin and effects of analogs on the growth of MCF-7 breast cancer cells. Mol. Pharmacol. 53 (1998) 62-67.

Graphical abstract